

Figure 3.8 -- Map showing hydro stratigraphy zones in model layer 6.

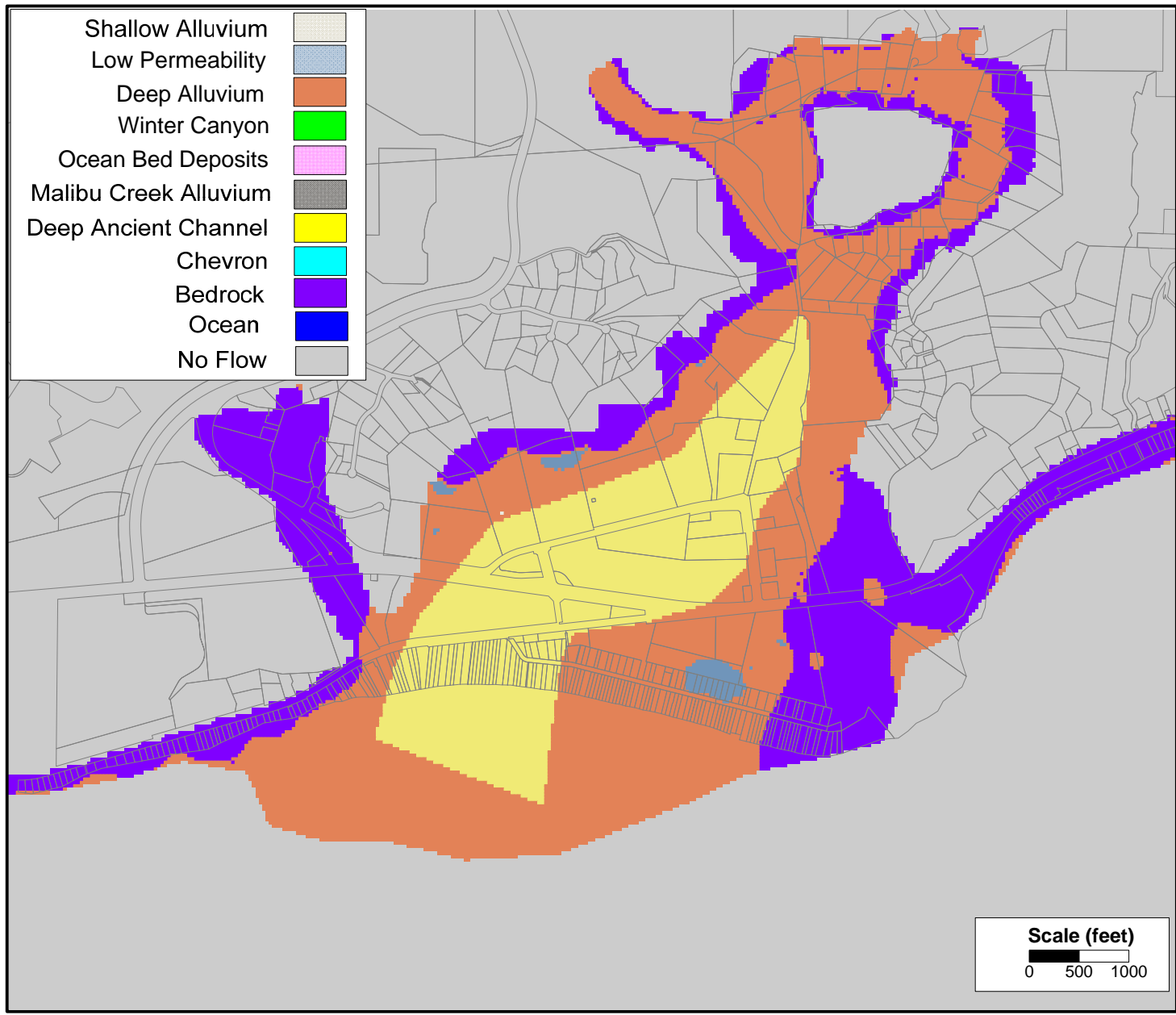


Figure 3.9 -- Map showing hydro stratigraphy zones in model layer 7.

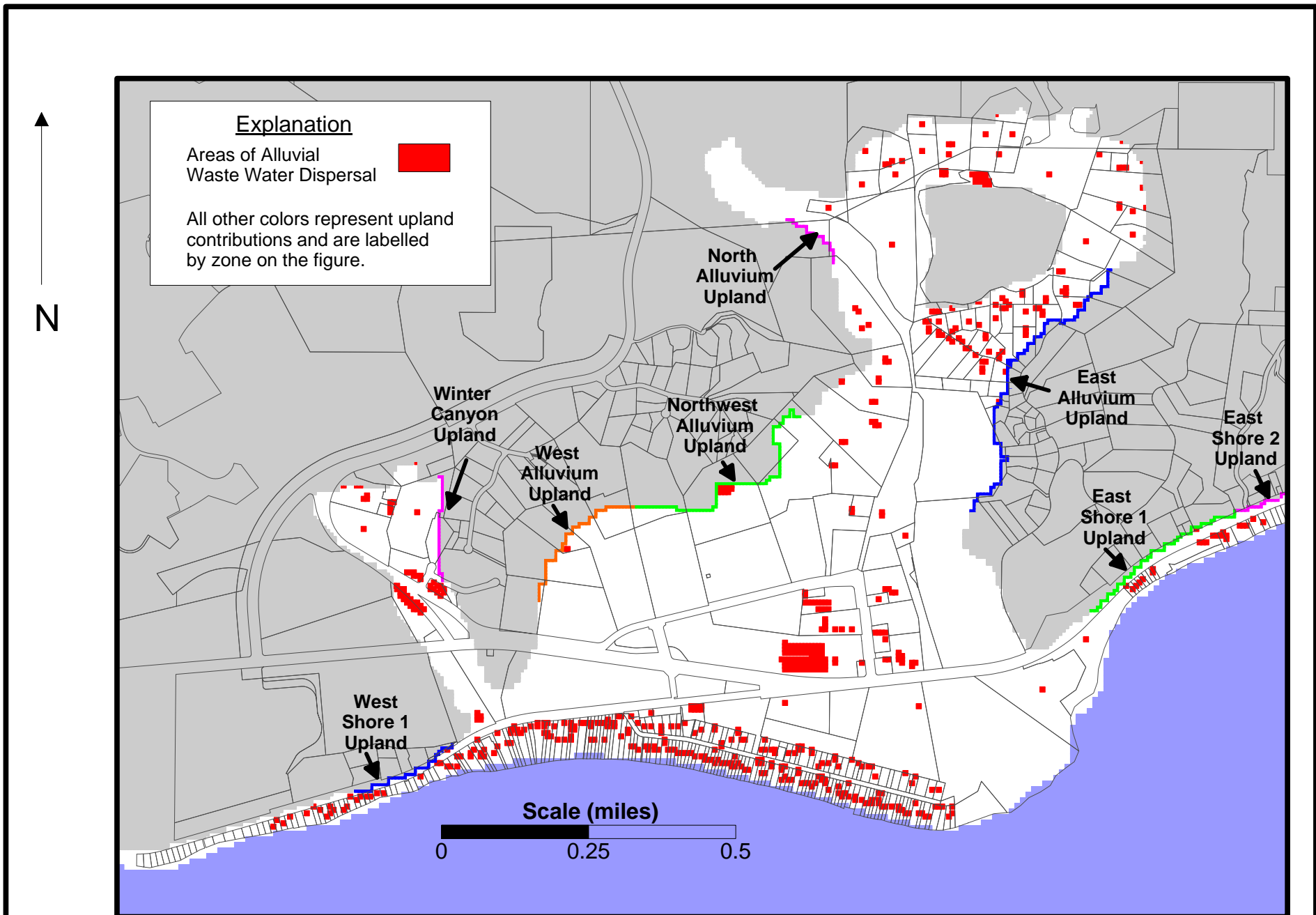


Figure 3.10 -- Map showing locations where subsurface waste water dispersal was simulated in the model using the WELL package in MODFLOW.

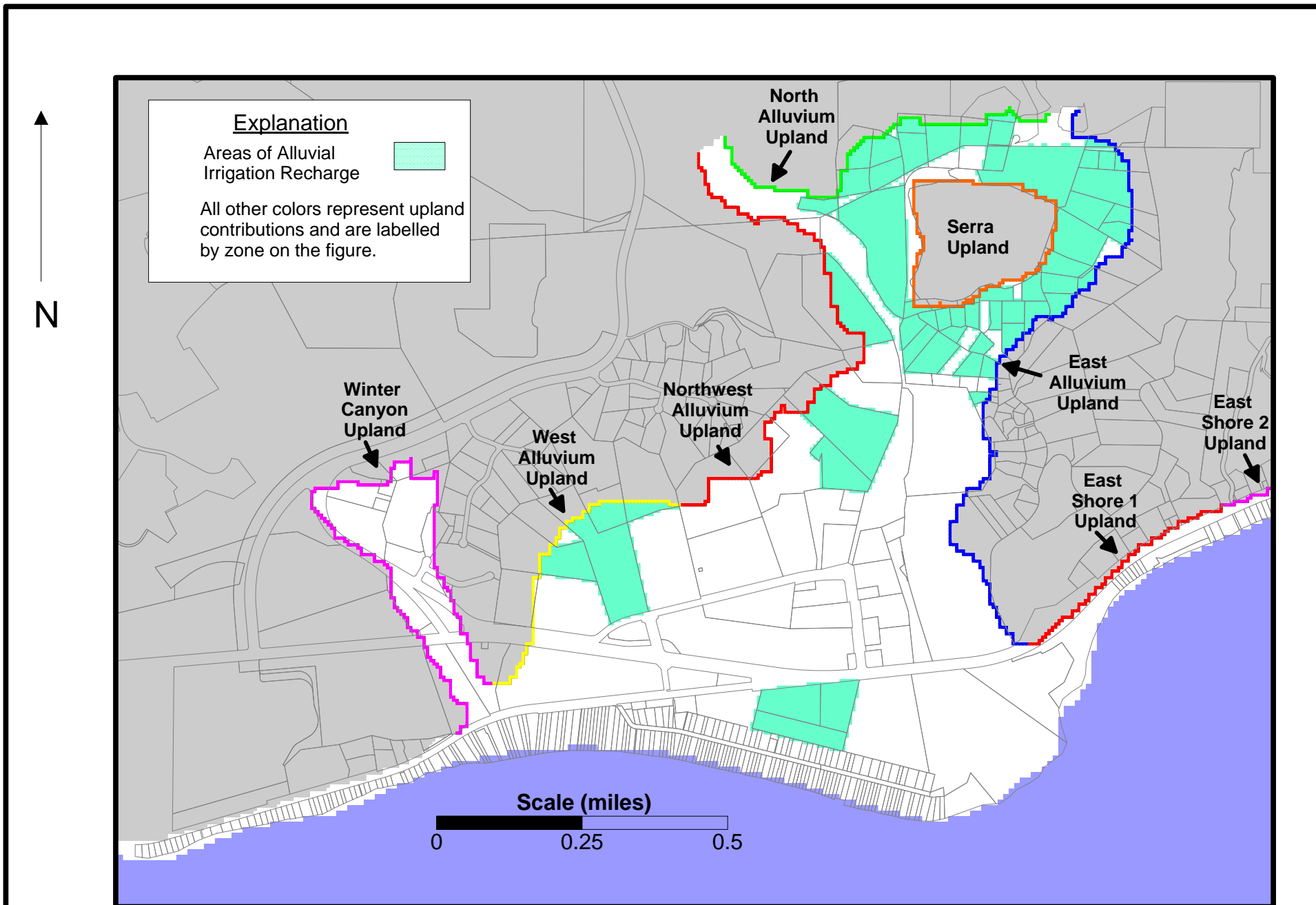


Figure 3.11 -- Map showing locations where recharge from excess irrigation was simulated in the model using the RIVER package in MODFLOW.

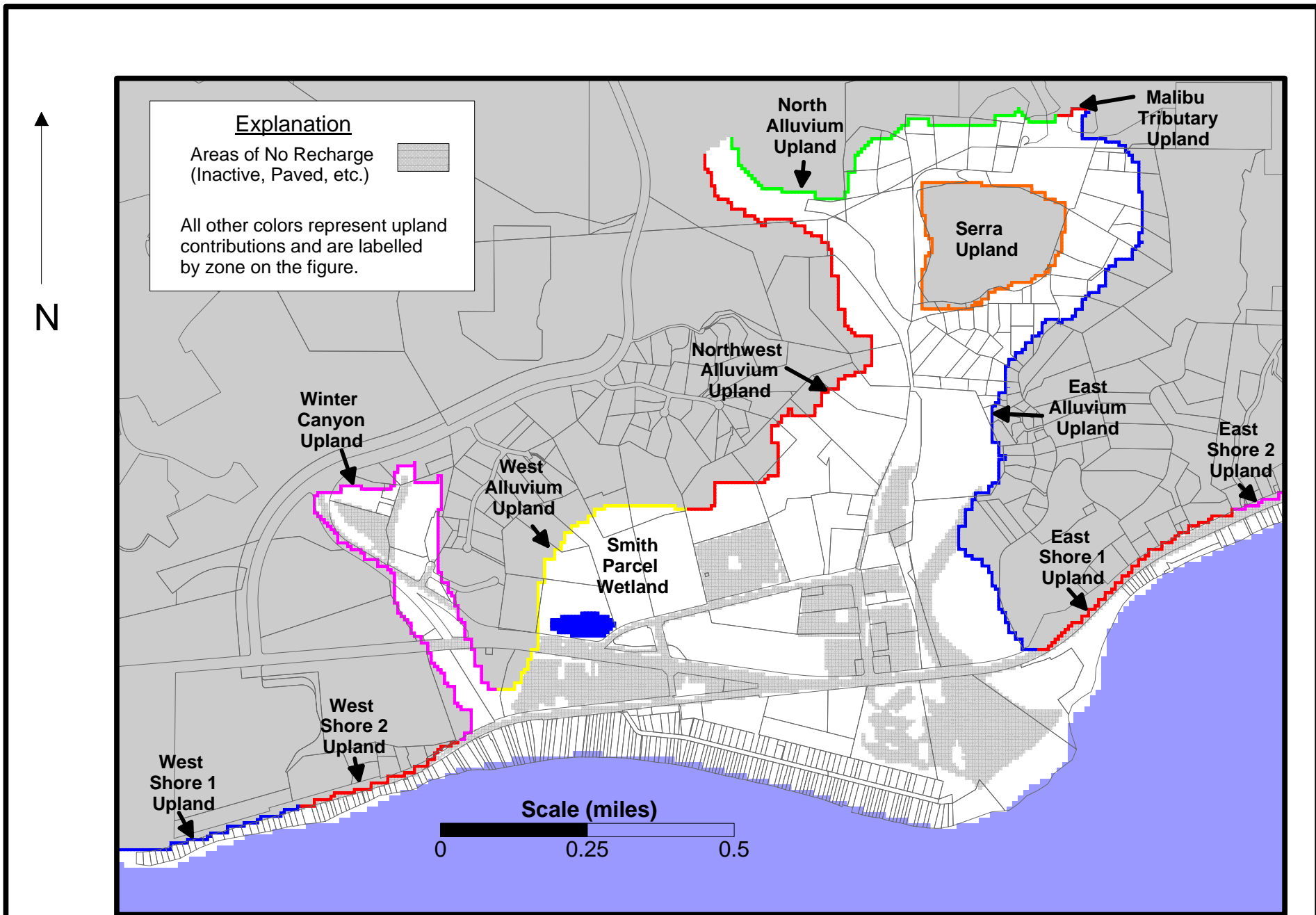


Figure 3.12 -- Map showing locations where recharge from infiltration of precipitation on the alluvial deposits and from runoff originating in upland areas was simulated in the model using the RECHARGE package in MODFLOW.

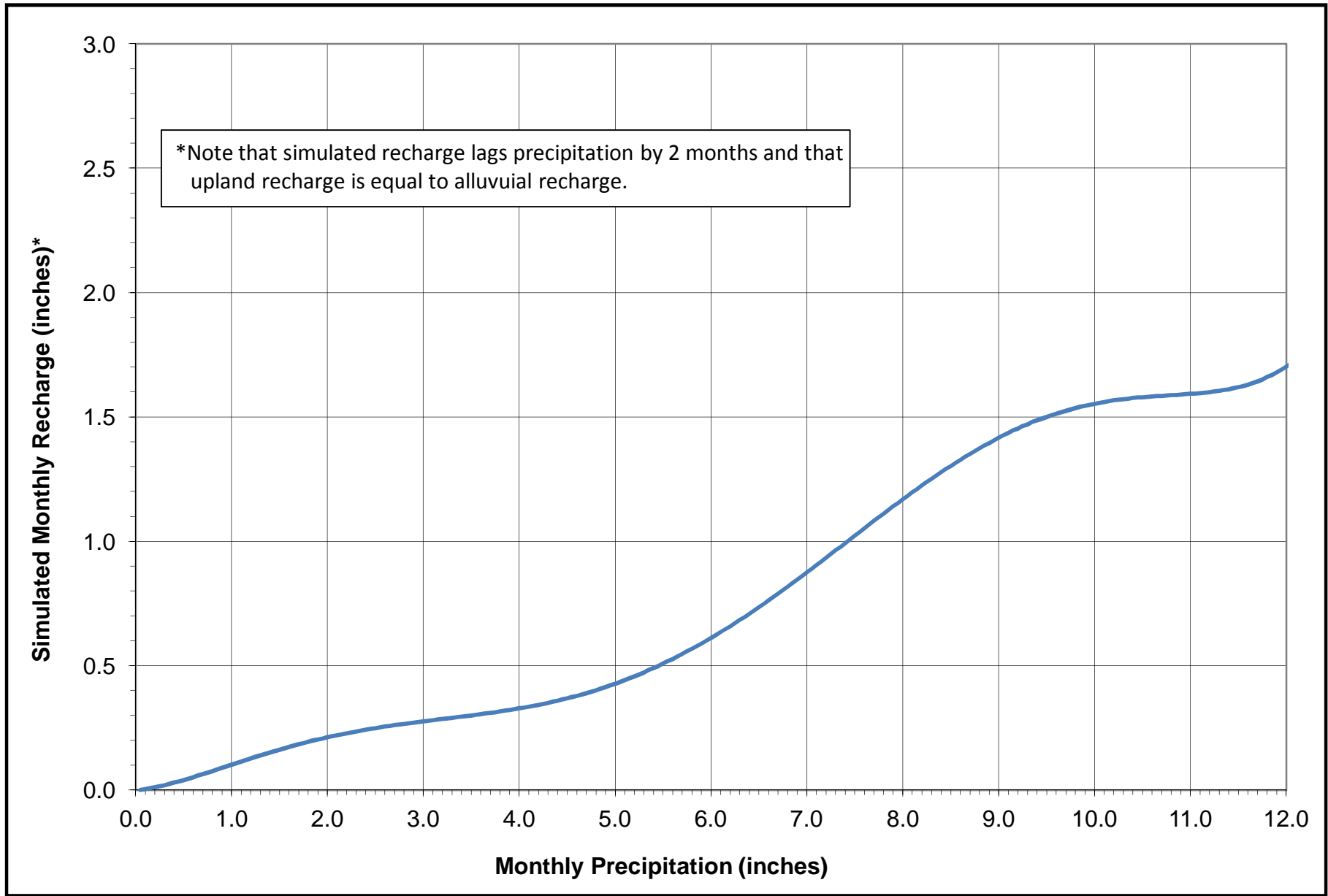


Figure 3.13. Graph showing simulated relationship between monthly precipitation and monthly recharge from infiltration of precipitation and upland runoff.

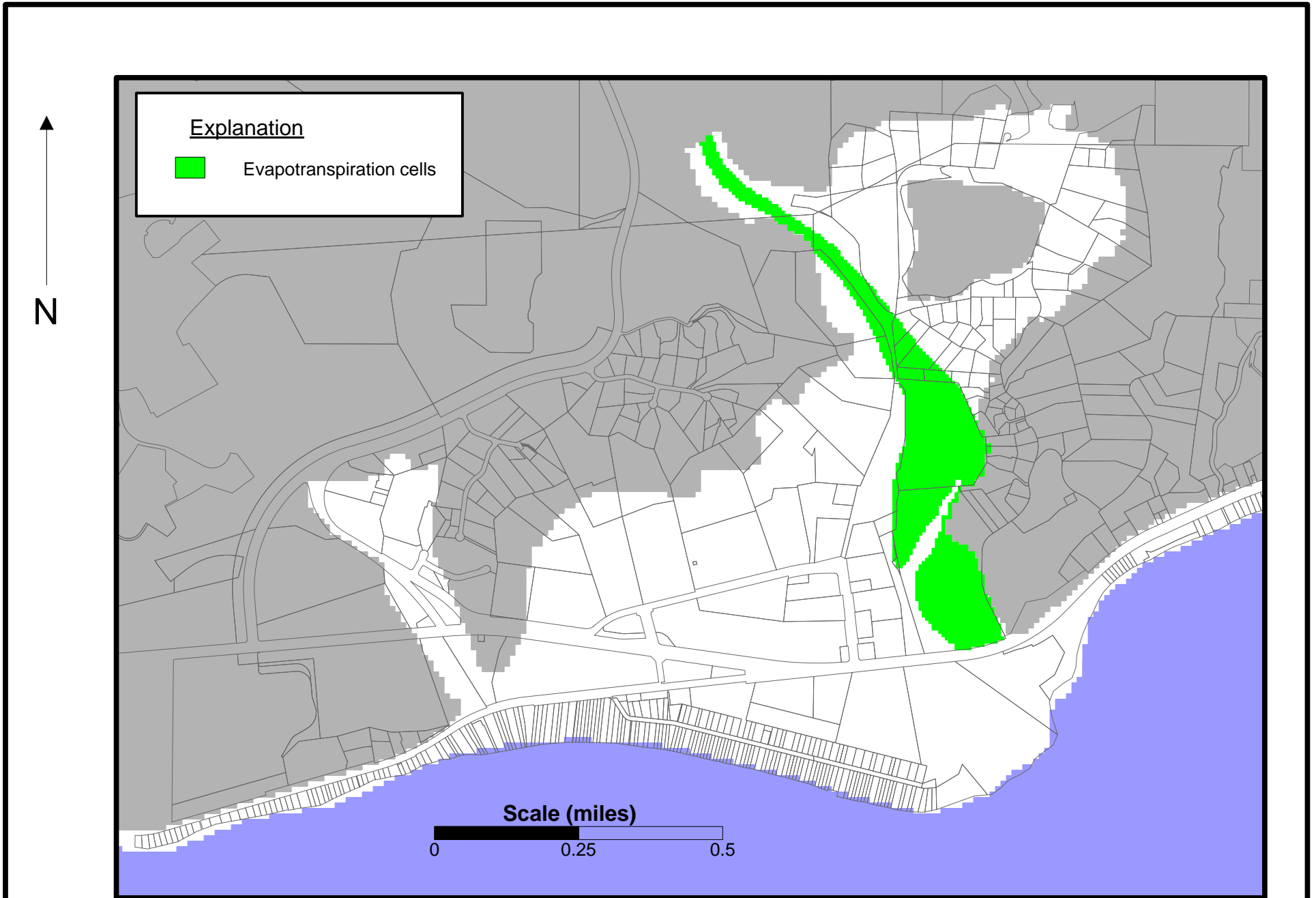
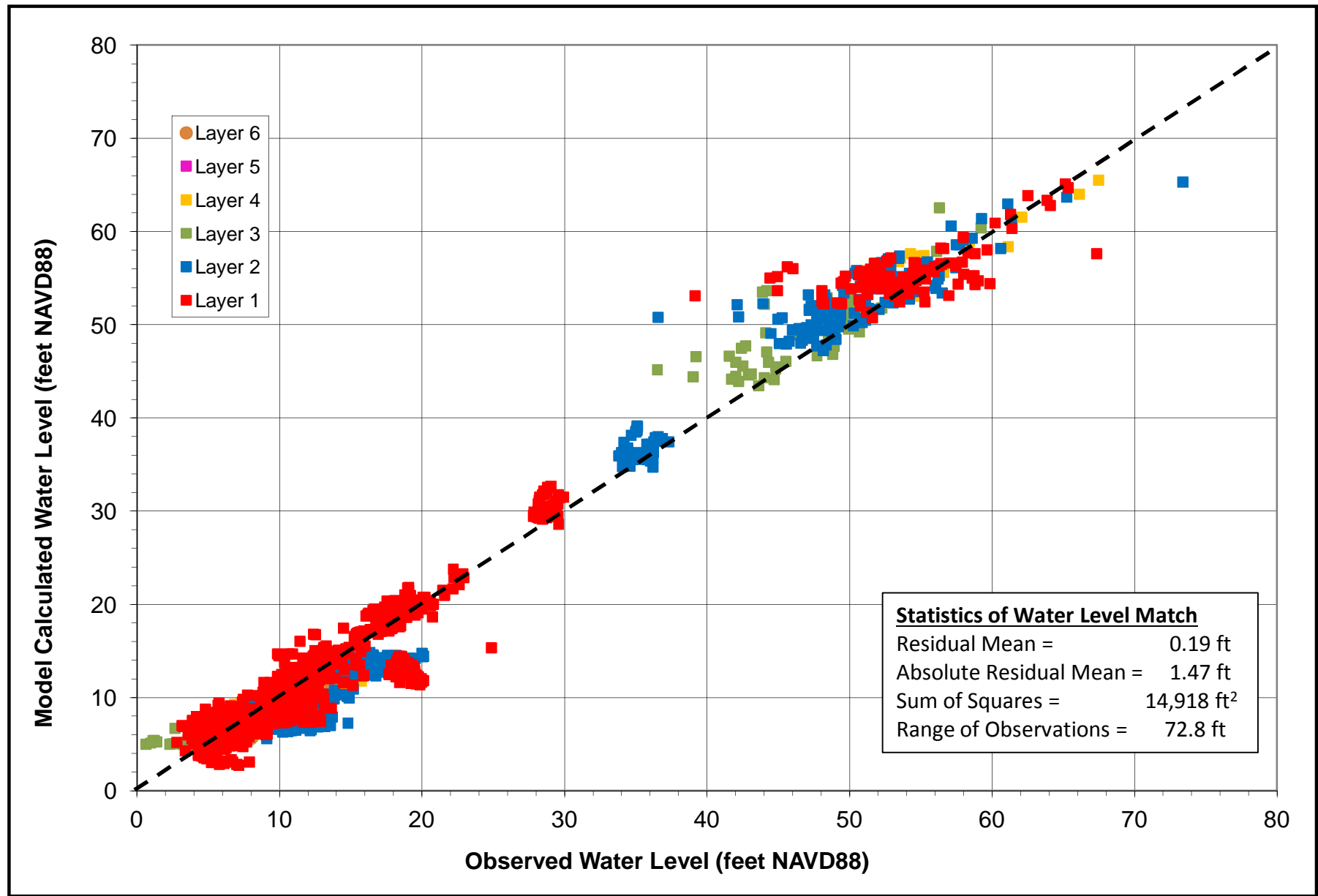


Figure 3.14 -- Map showing locations where groundwater evapotranspiration was simulated in the model with the ET package in MODFLOW.



Run: malibu_phase3_pest_13014

Figure 3.15 -- Scatter plot showing comparison of model calculated water levels with observed water levels.

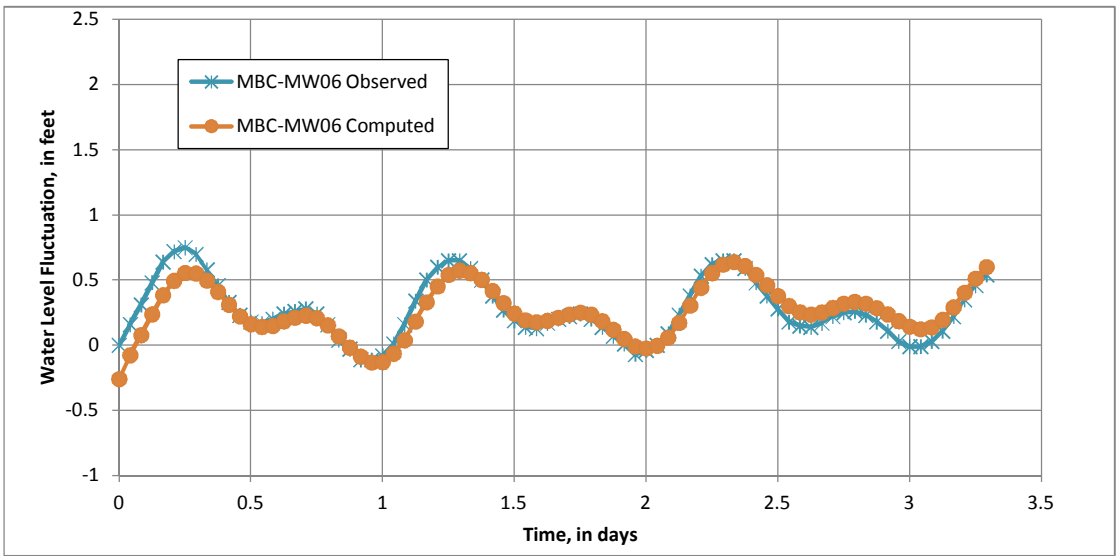
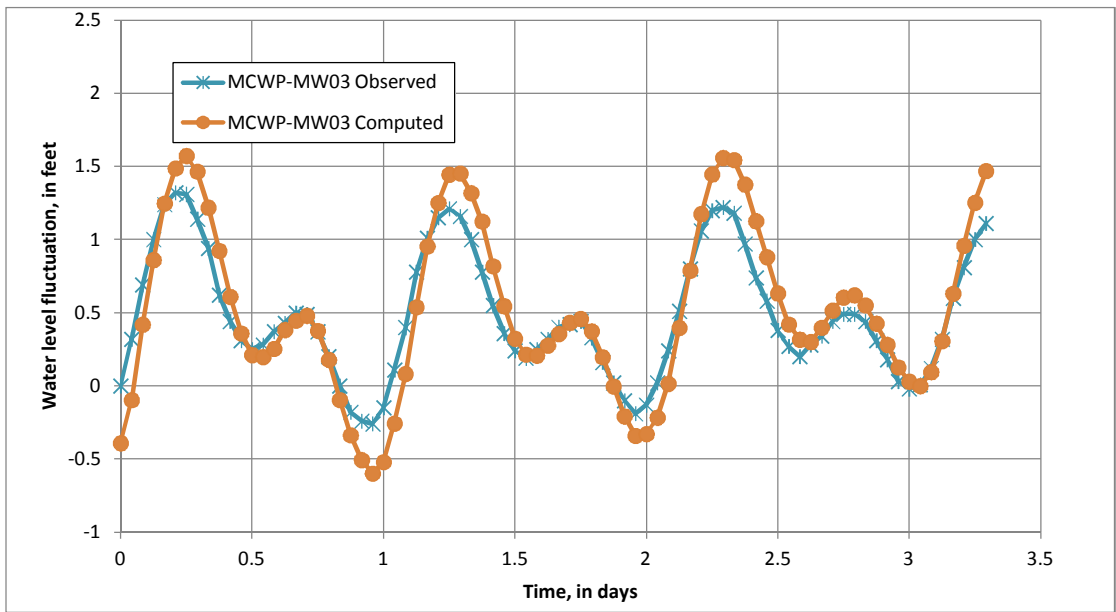


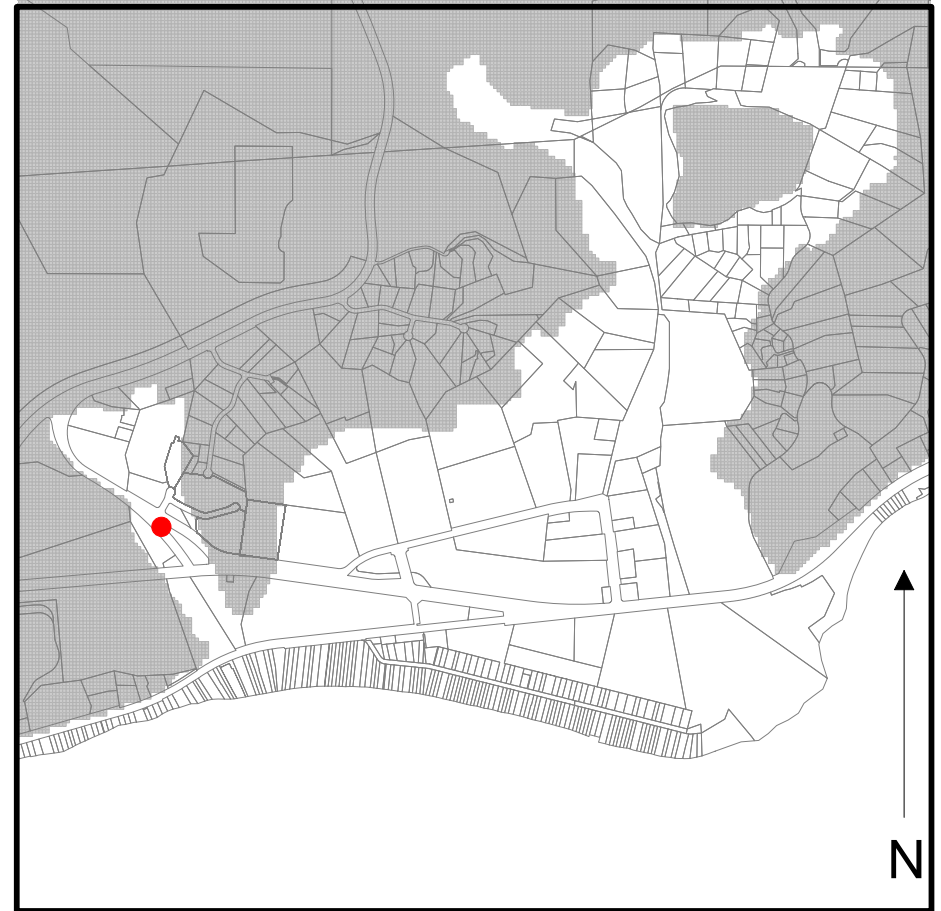
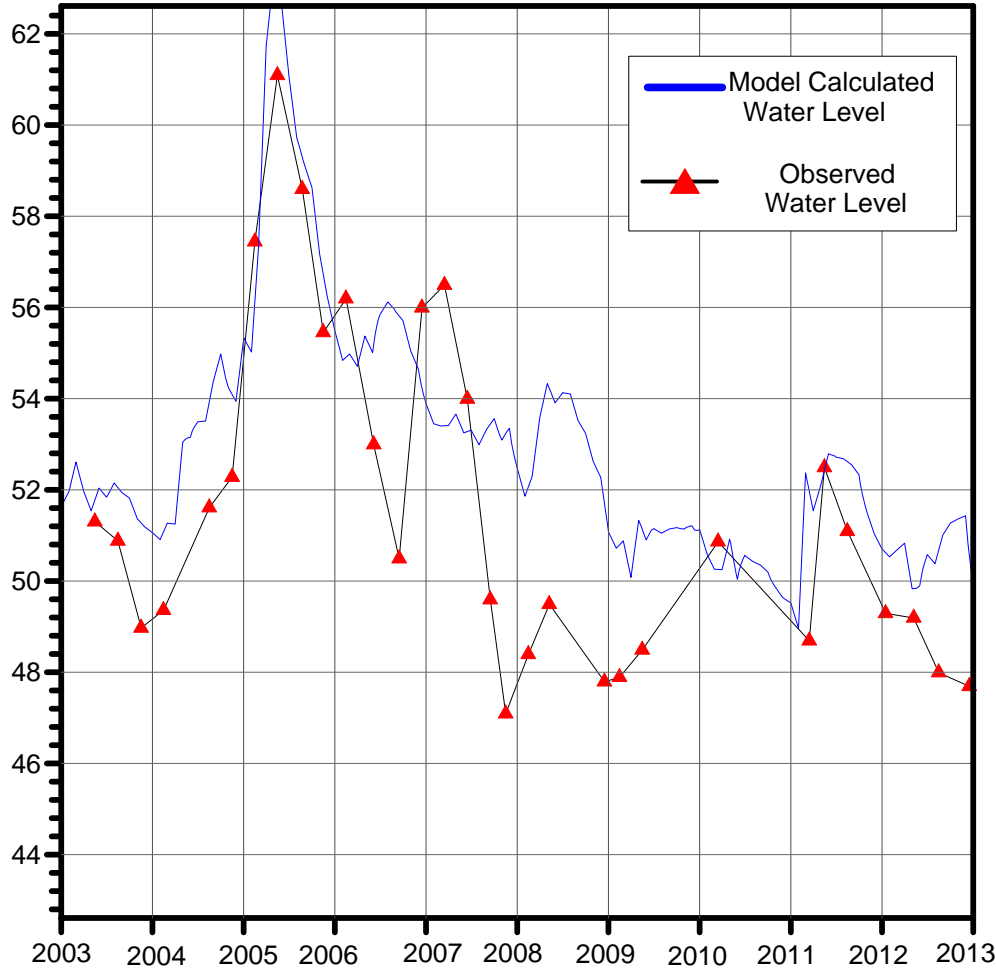
Figure 3.16 -- Graphs showing model calculated and observed tidal fluctuations at wells MCWP-MW03 and MBC-MW06.

Malibu Hydrograph

Well02_4458028020

Water Level Elevation (ft msl NAVD88)

Model Layer 2



Number of Target Water Levels 31
Range of Elevation 47.09 to 61.09
Average Elevation 51.58

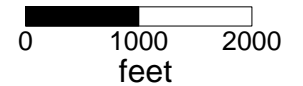
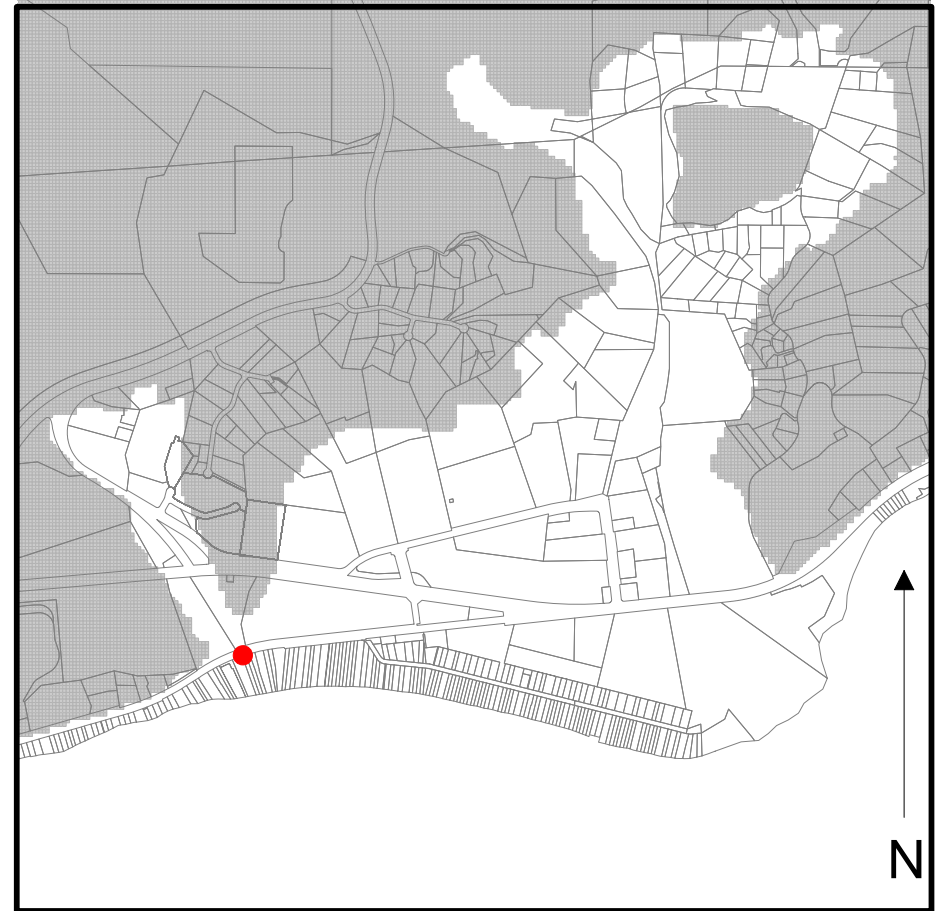
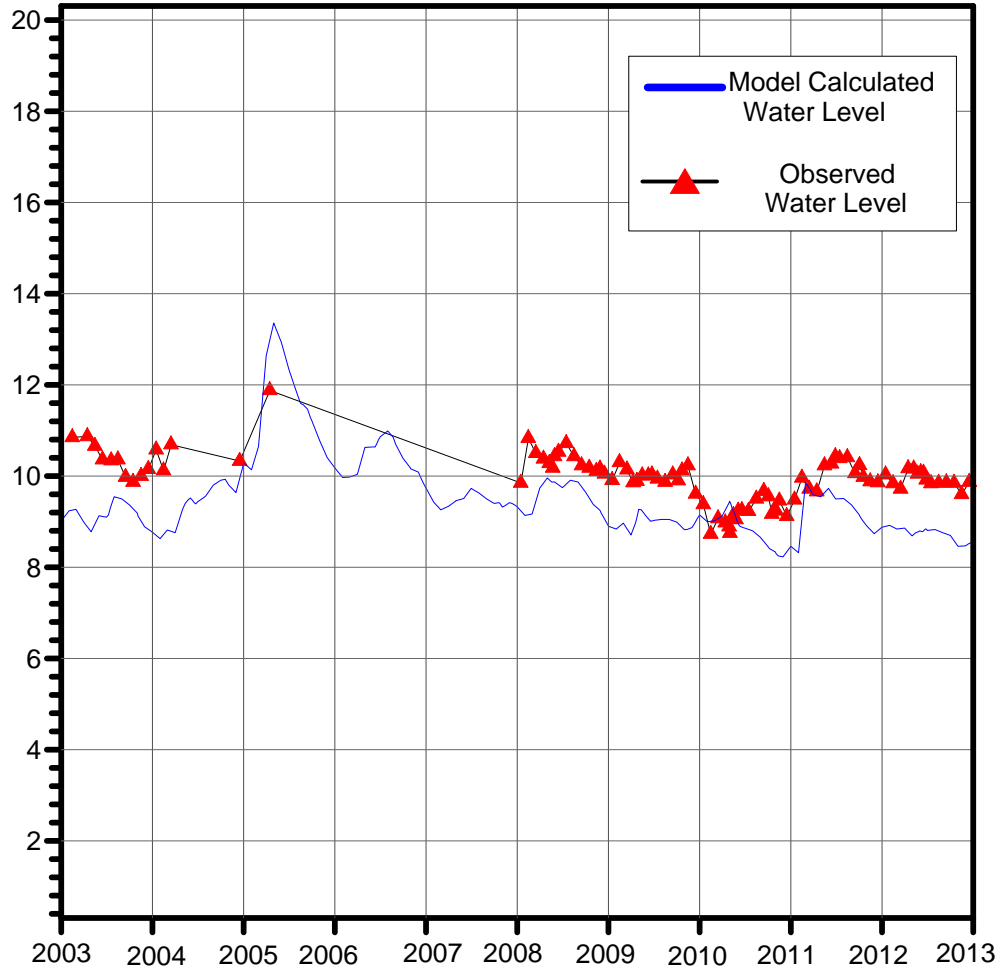
Figure 3.17a. Hydrograph showing model calculated and observed water levels at well Well02.

Malibu Hydrograph

SMBRP-11_4458007018

Water Level Elevation (ft msl NAVD88)

Model Layer 1



Number of Target Water Levels	94
Range of Elevation	8.73 to 11.88
Average Elevation	9.95

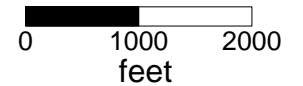
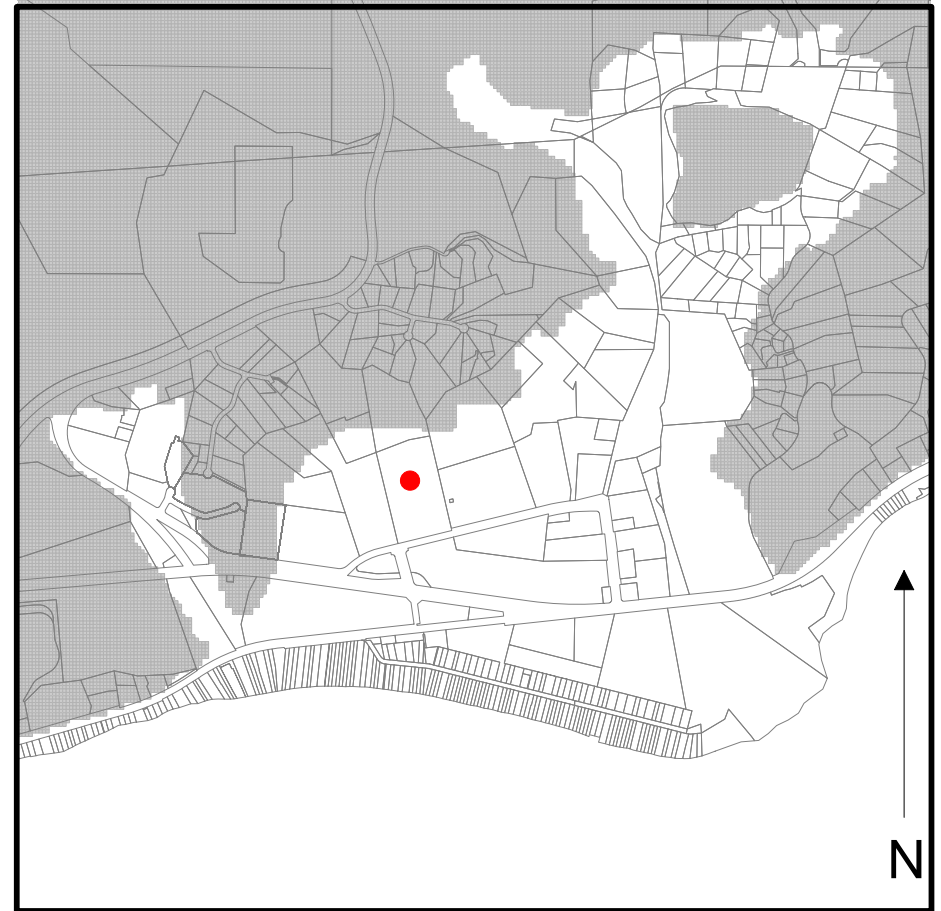
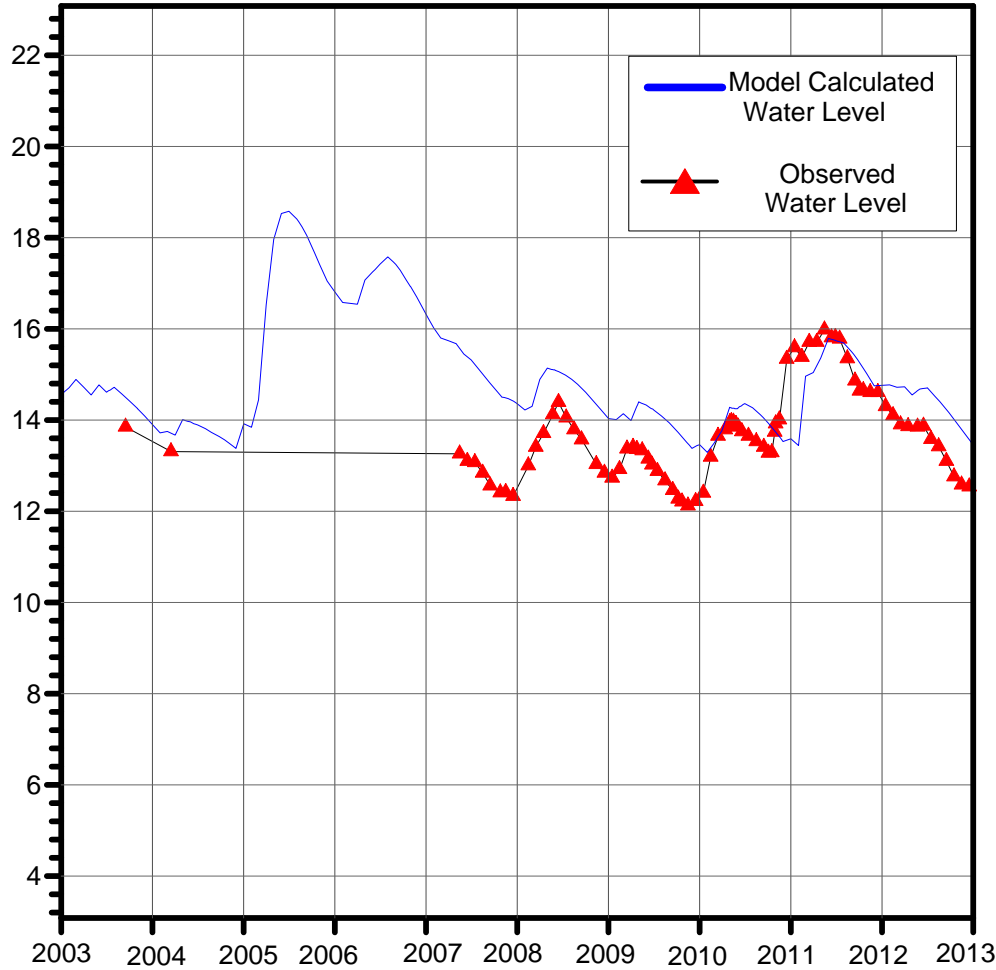
Figure 3.17b. Hydrograph showing model calculated and observed water levels at well SMBRP-11.

Malibu Hydrograph

MW-5_4458022011

Water Level Elevation (ft msl NAVD88)

Model Layer 1



Number of Target Water Levels 81
Range of Elevation 12.12 to 15.98
Average Elevation 13.68

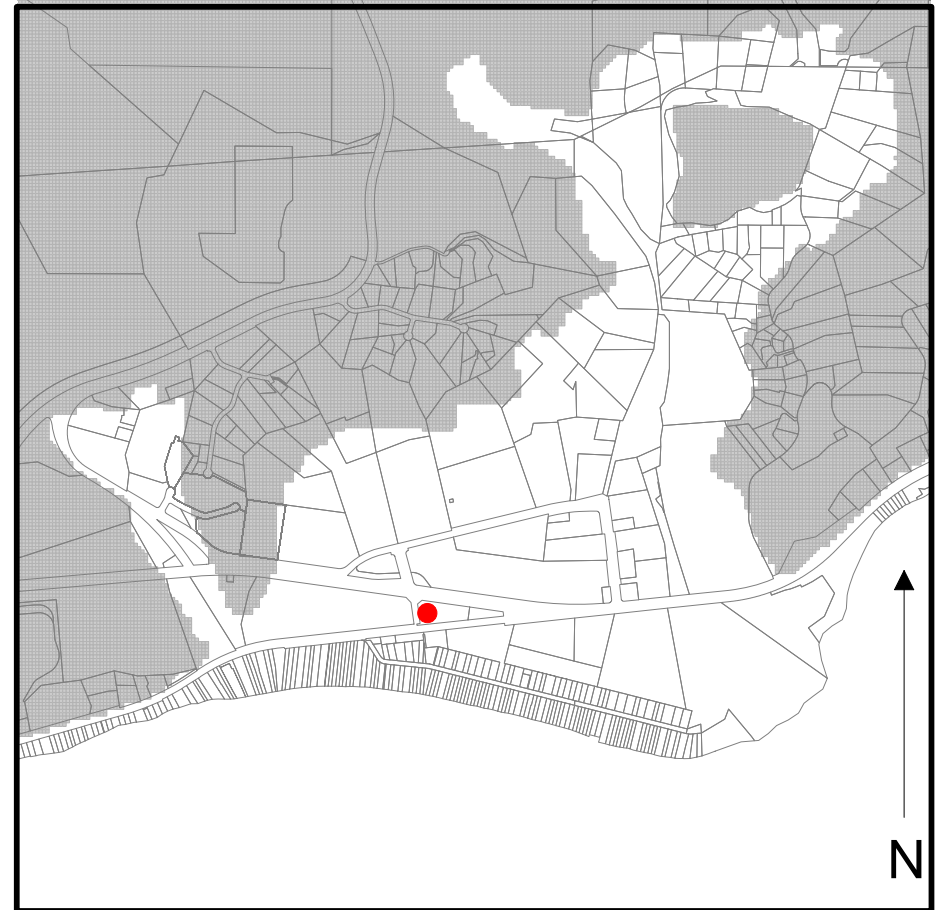
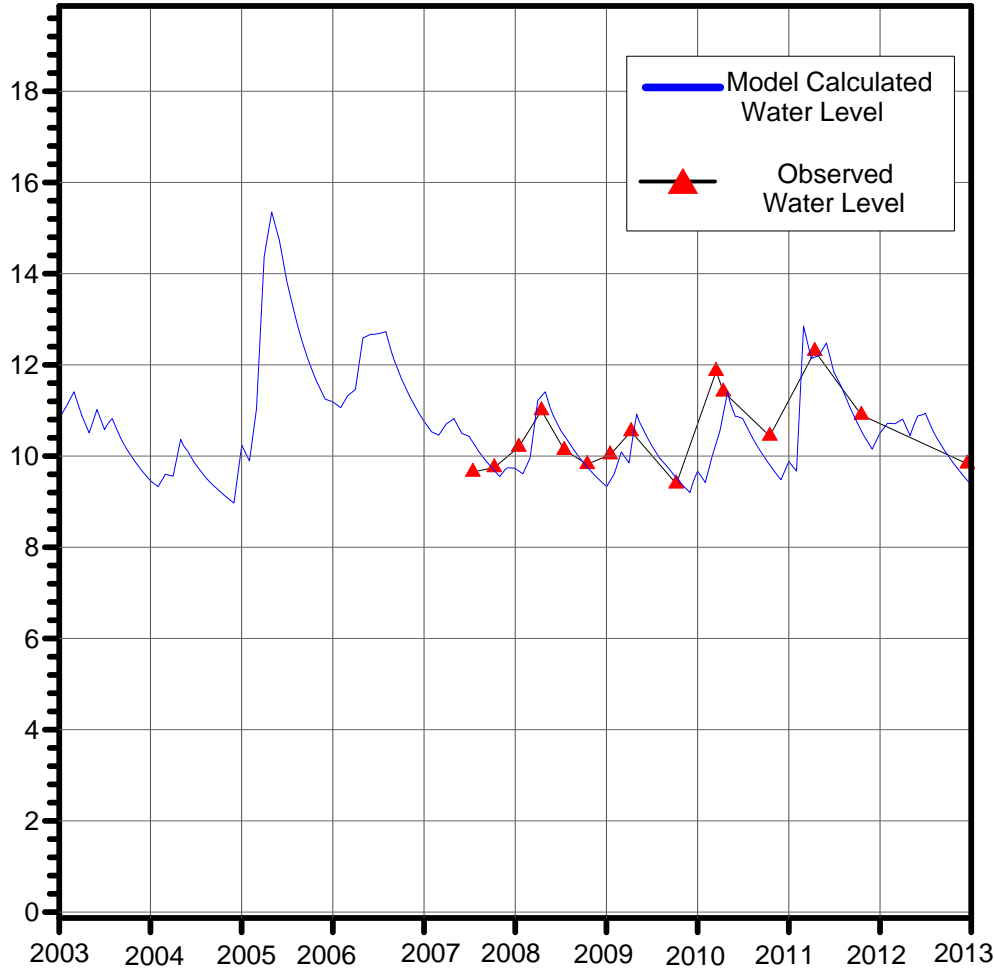
Figure 3.17c. Hydrograph showing model calculated and observed water levels at well MW-5.

Malibu Hydrograph

W-4A_4458019006

Water Level Elevation (ft msl NAVD88)

Model Layer 1



Number of Target Water Levels 15
Range of Elevation 9.39 to 12.30
Average Elevation 10.48

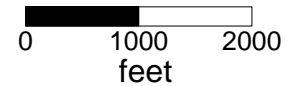
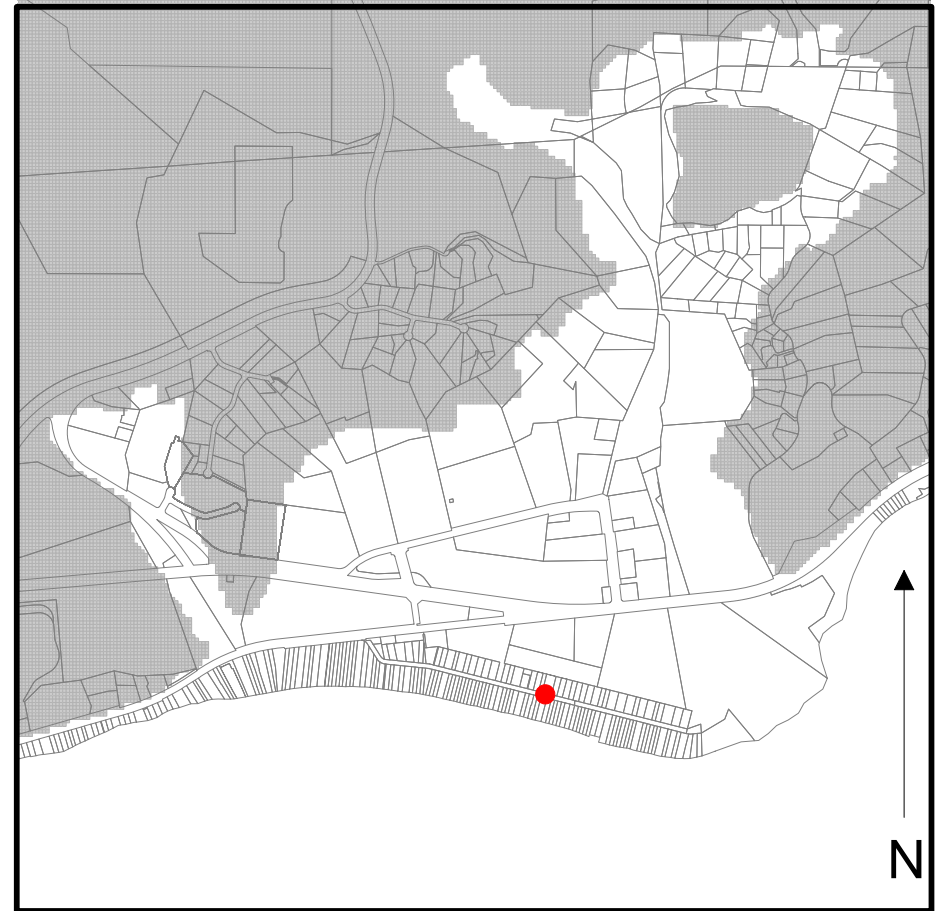
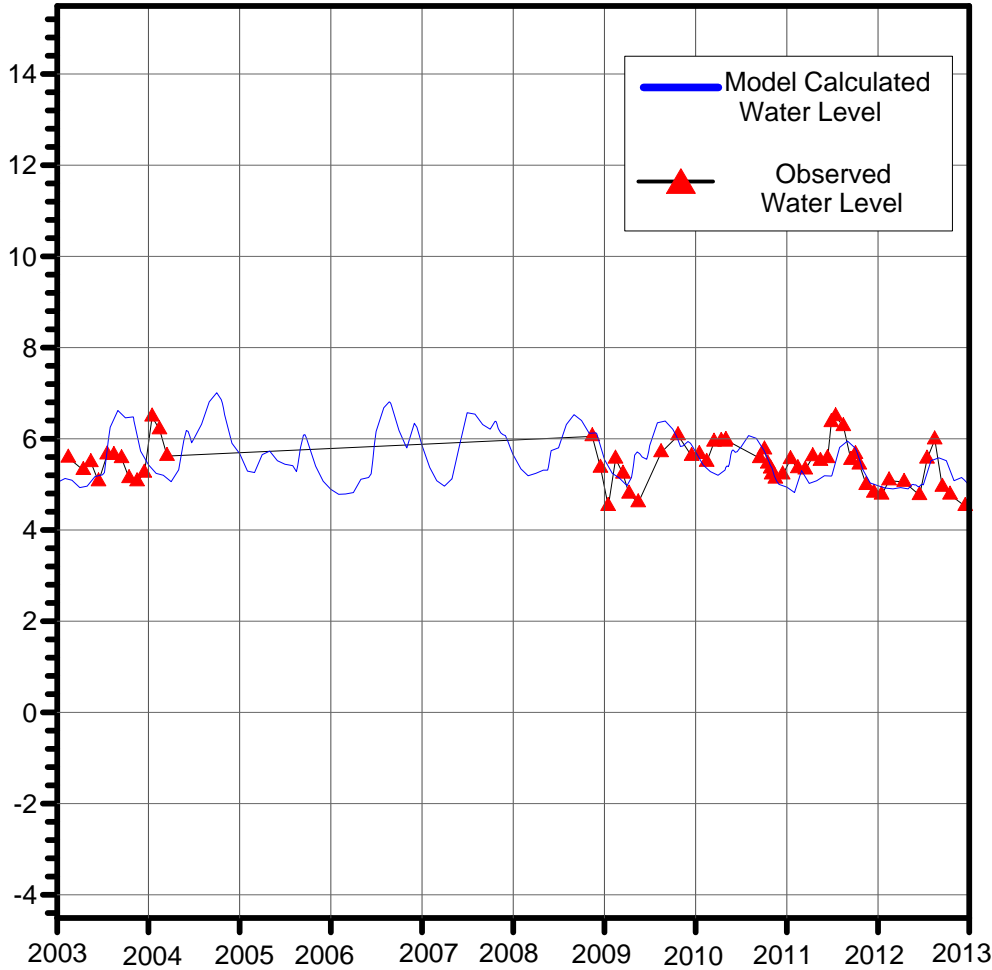
Figure 3.17d. Hydrograph showing model calculated and observed water levels at well W-4A.

Malibu Hydrograph

SMBRP-13_4458001002

Water Level Elevation (ft msl NAVD88)

Model Layer 1



Number of Target Water Levels	59
Range of Elevation	4.52 to 6.49
Average Elevation	5.46

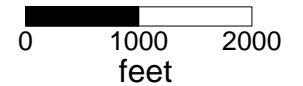
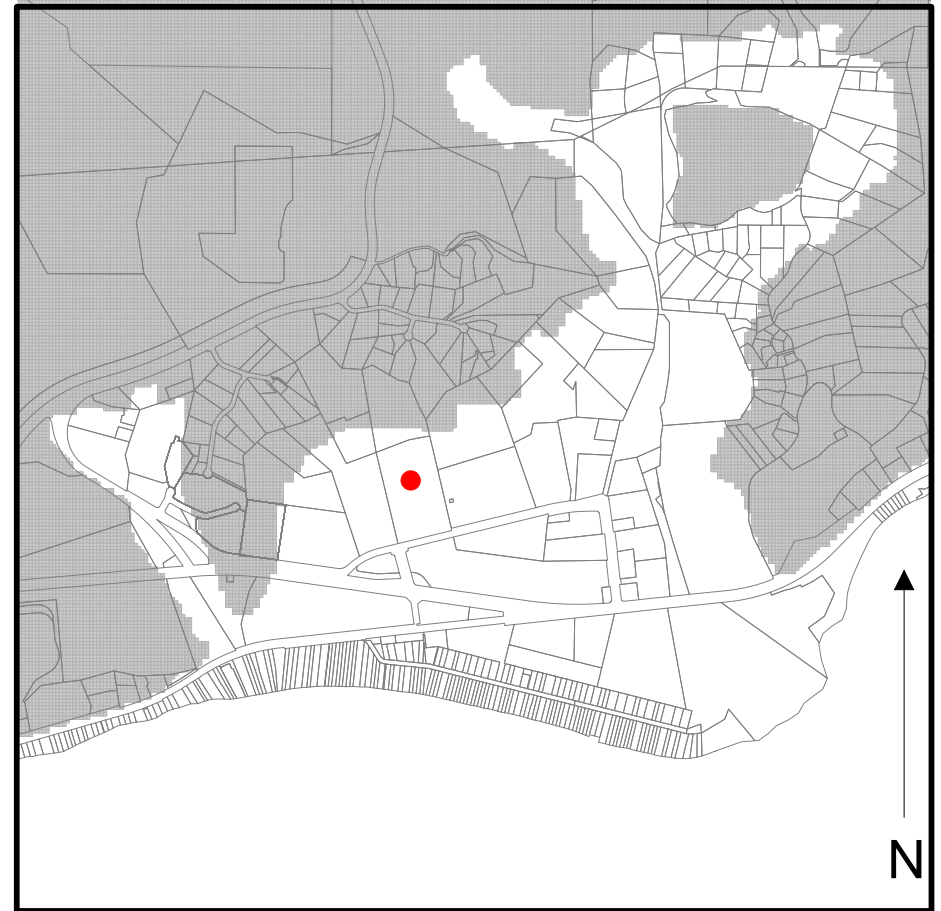
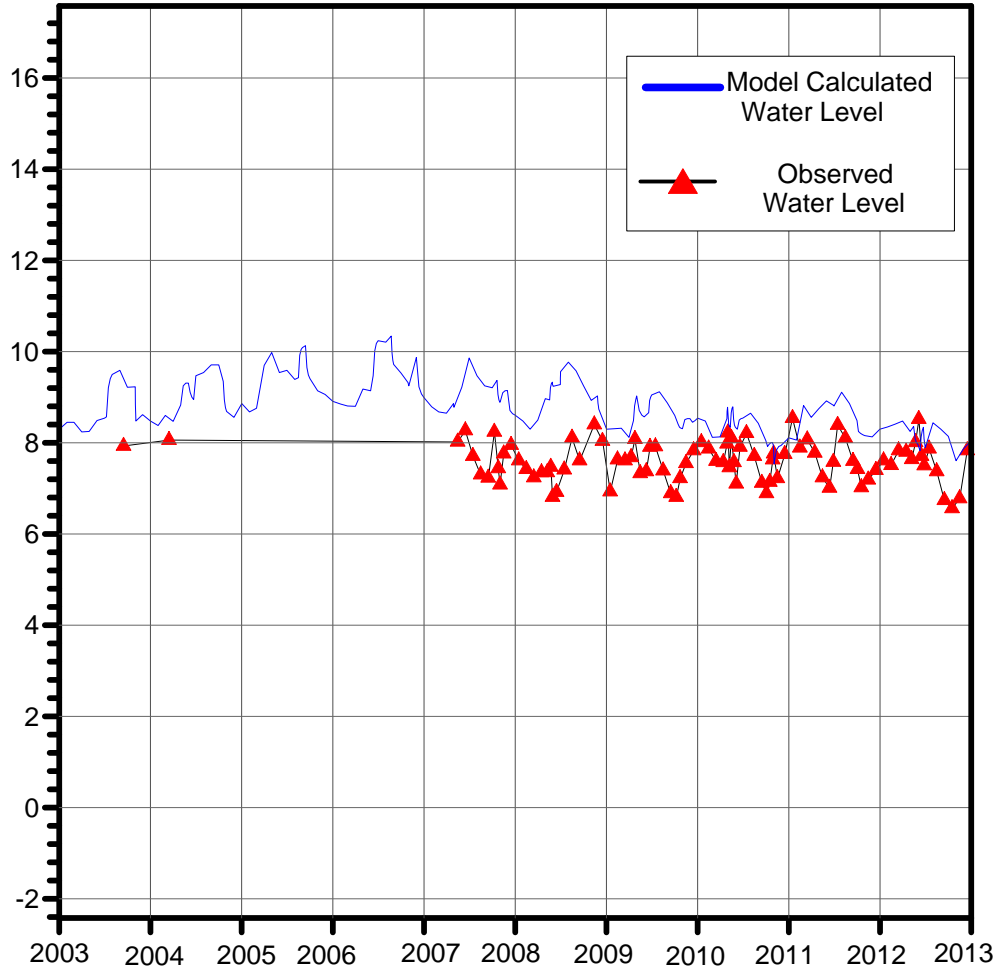
Figure 3.17e. Hydrograph showing model calculated and observed water levels at well SMBRP-13.

Malibu Hydrograph

MW-6_4458022011

Water Level Elevation (ft msl NAVD88)

Model Layer 4



Number of Target Water Levels 89
Range of Elevation 6.56 to 8.54
Average Elevation 7.60

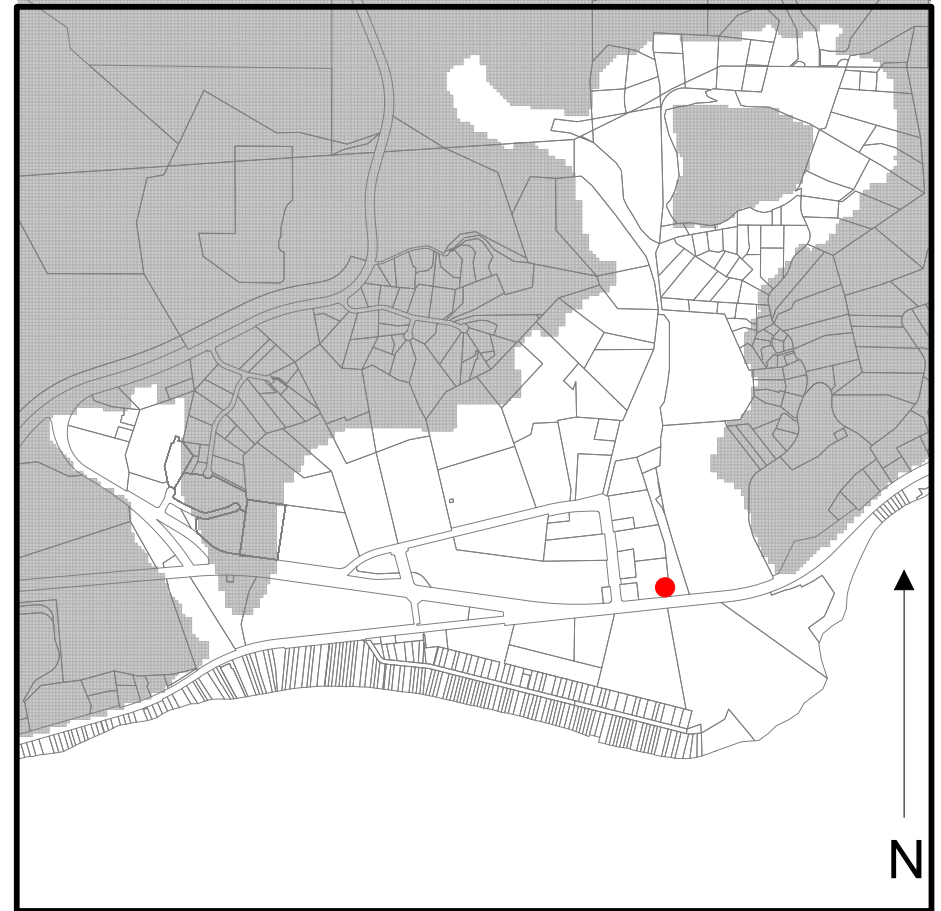
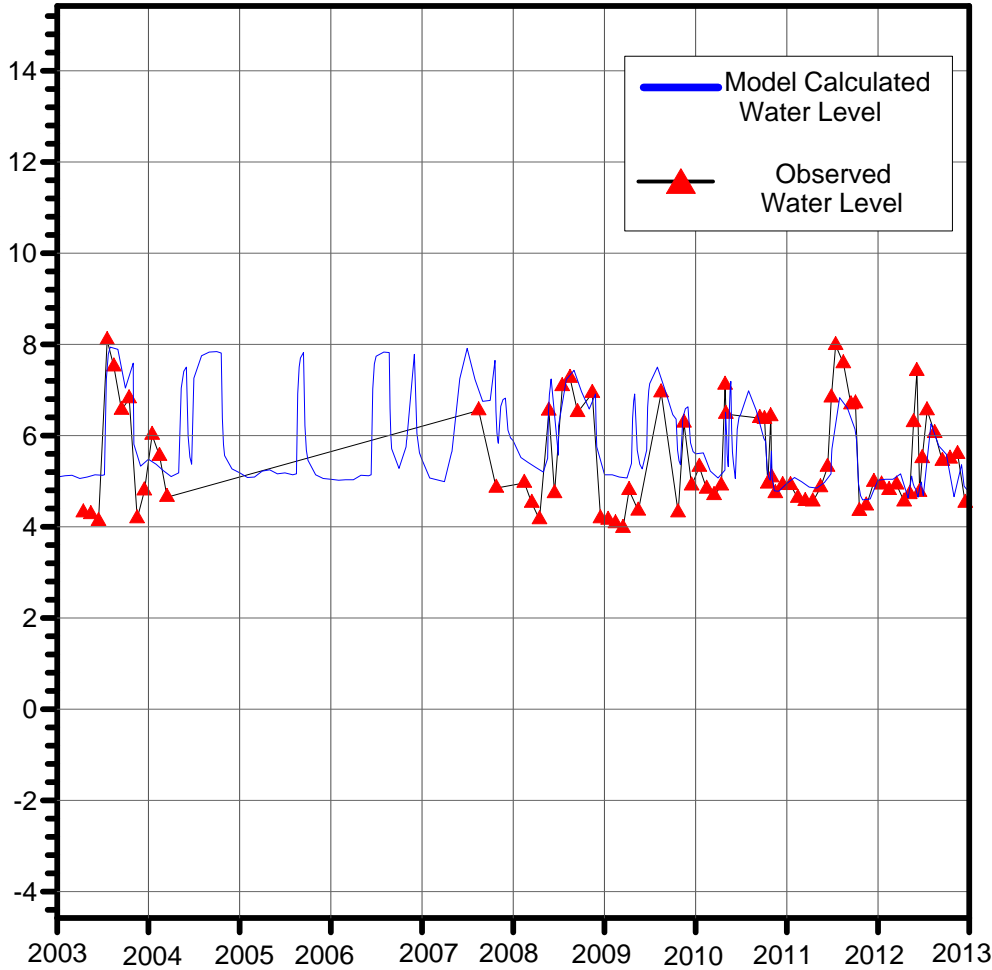
Figure 3.17f. Hydrograph showing model calculated and observed water levels at well MW-6.

Malibu Hydrograph

P-9_4452011043

Water Level Elevation (ft msl NAVD88)

Model Layer 1



Number of Target Water Levels 75
Range of Elevation 3.97 to 8.09
Average Elevation 5.48

Figure 3.17g. Hydrograph showing model calculated and observed water levels at well P-9.

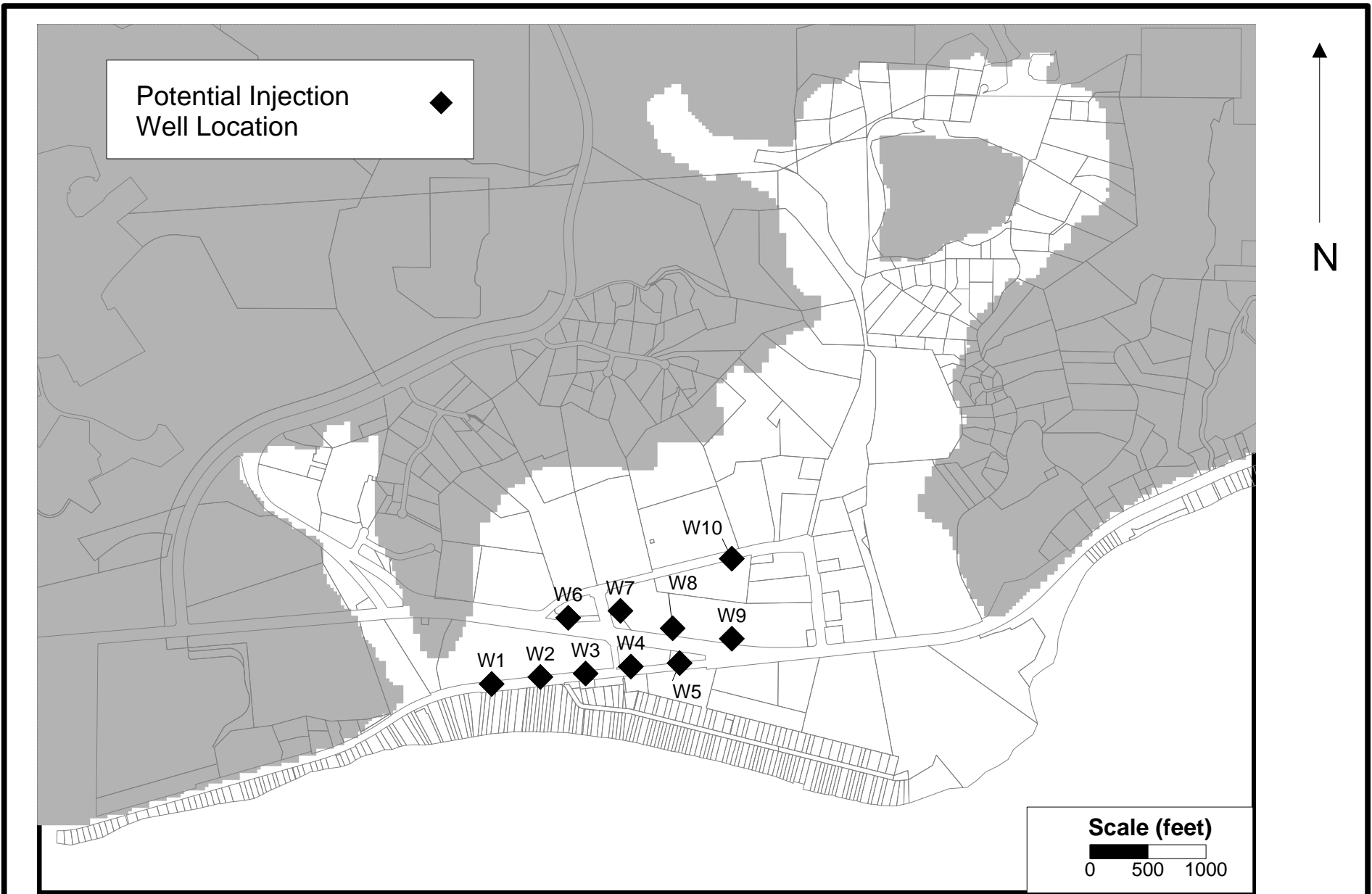


Figure 3.18 - Map showing location of potential injection wells used in the optimization process.

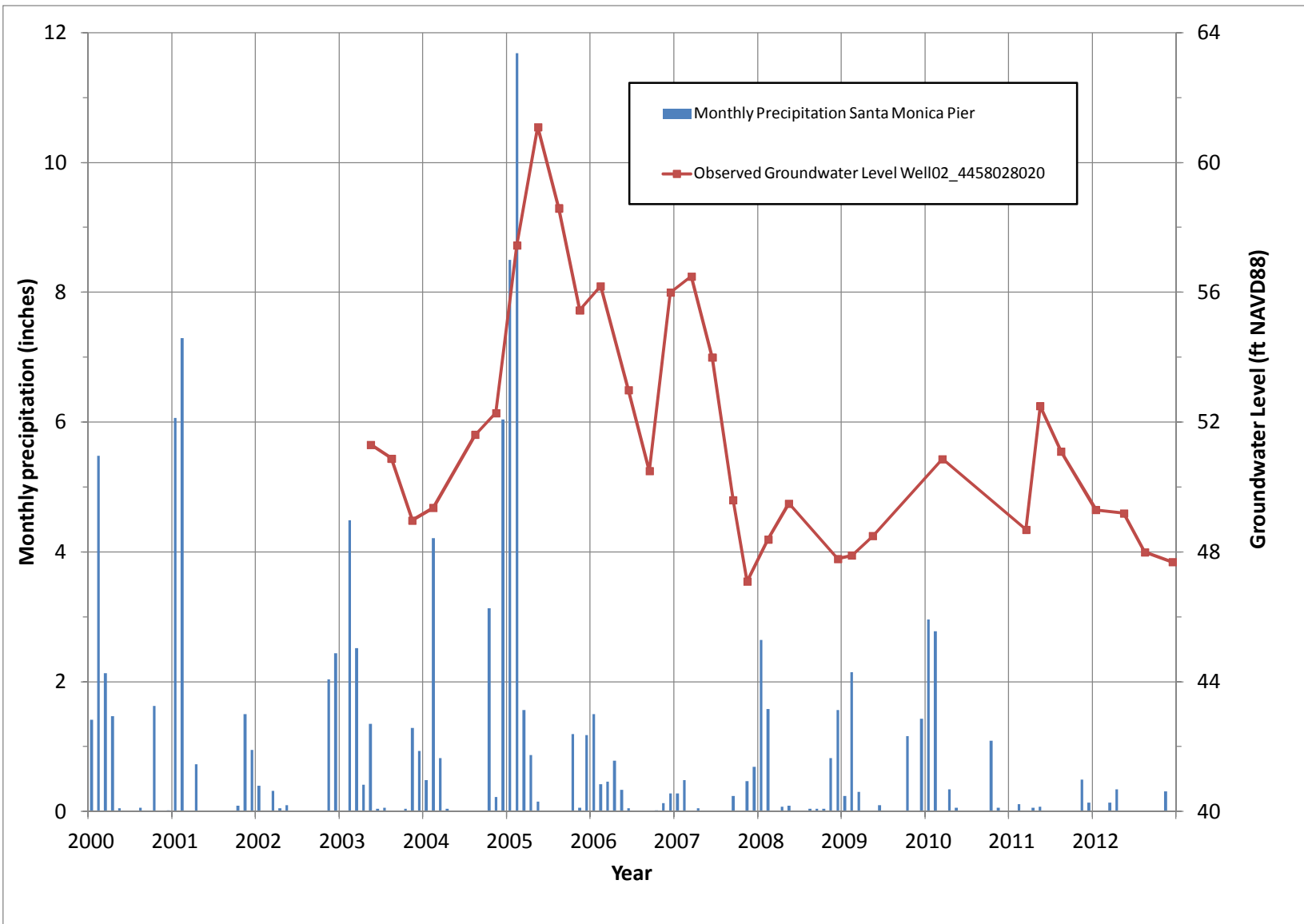


Figure 3.20 - Hydrograph showing groundwater levels from a well in Winter Canyon and monthly precipitation at Santa Monica Pier.

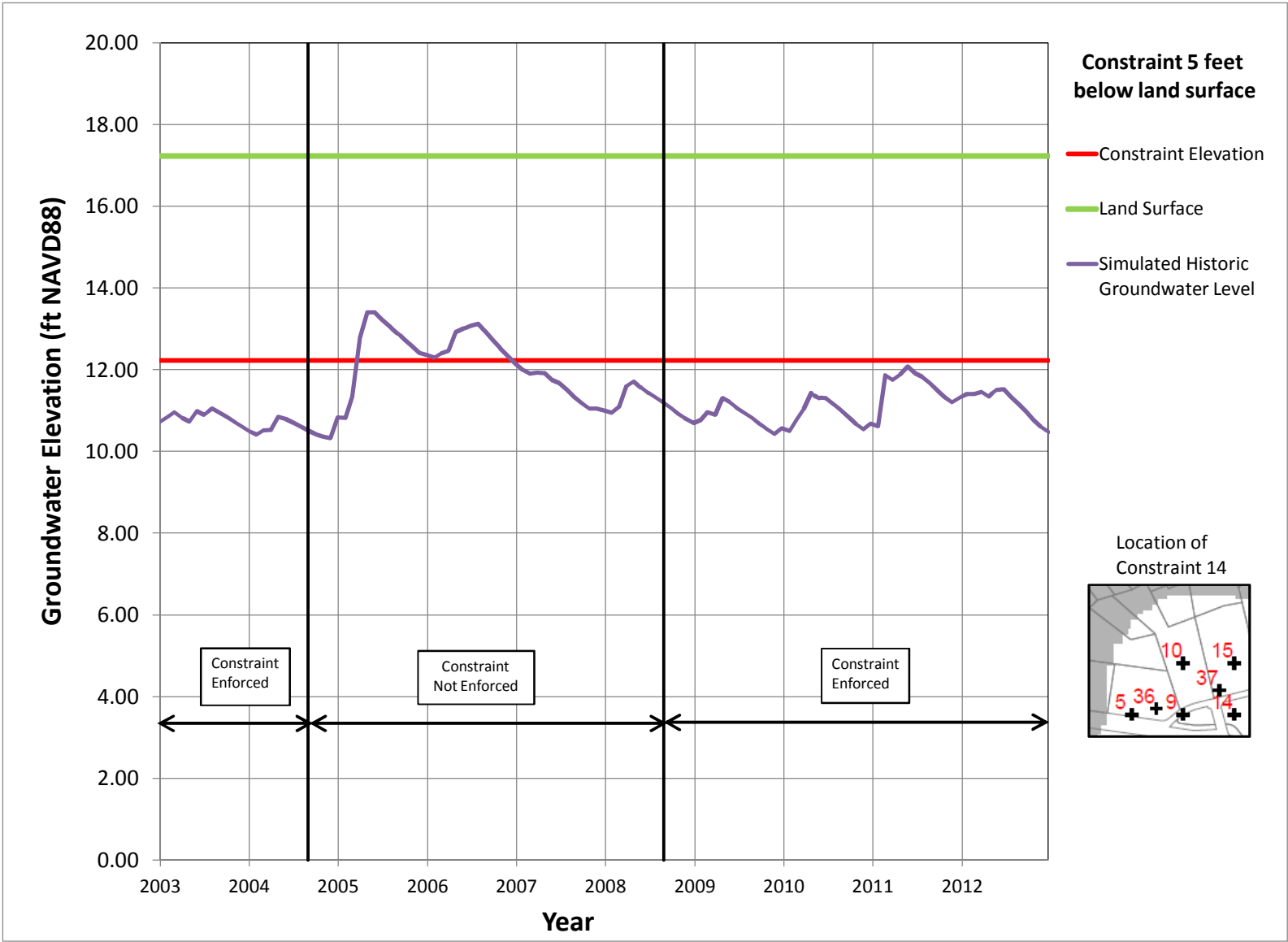


Figure 3.21 Hydrograph showing elevations of land surface, groundwater level constraint, and simulated historic groundwater levels at constraint 14.

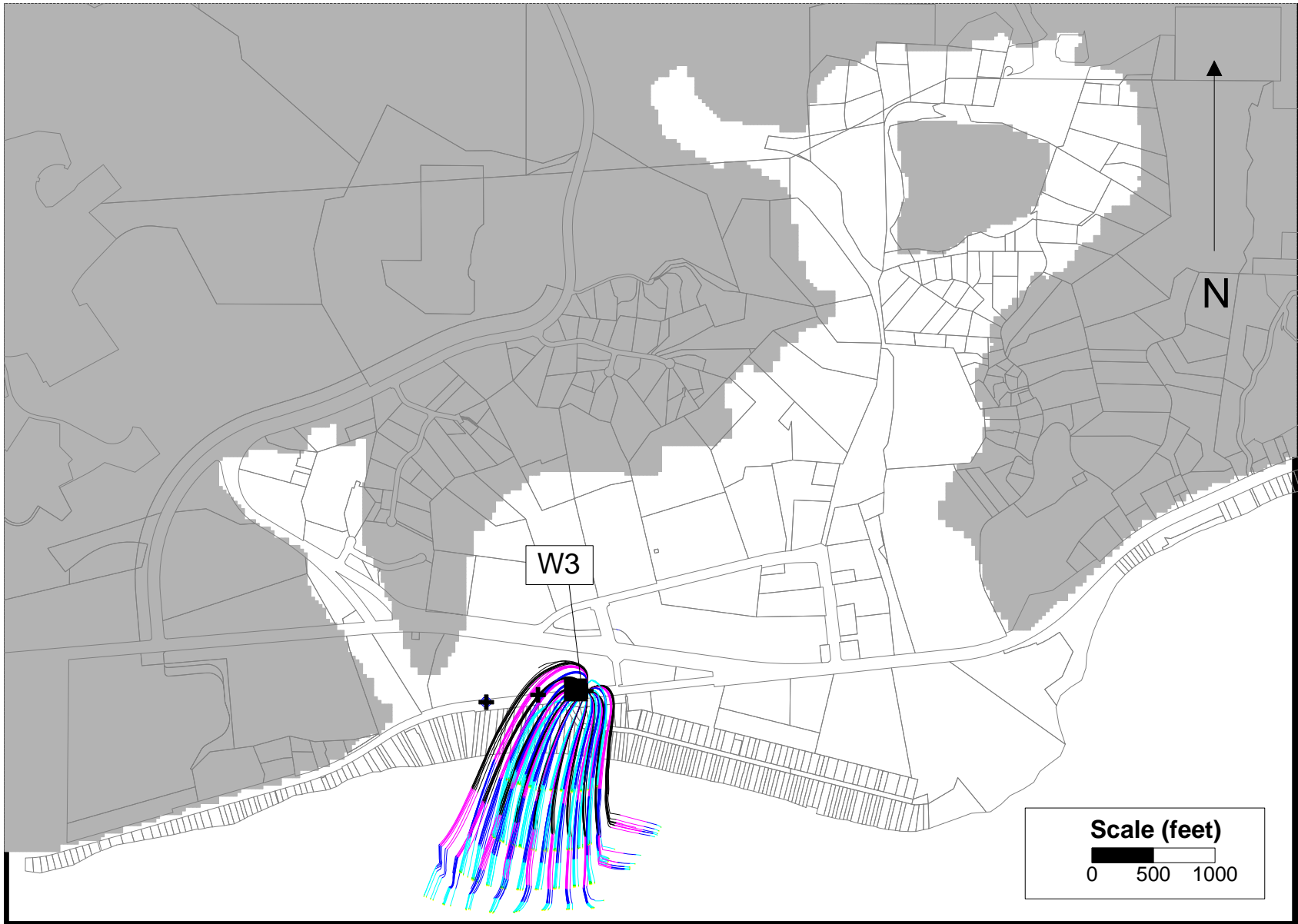


Figure 3.22 - Particle tracking from optimized injection sites representing Phase 1 conditions.

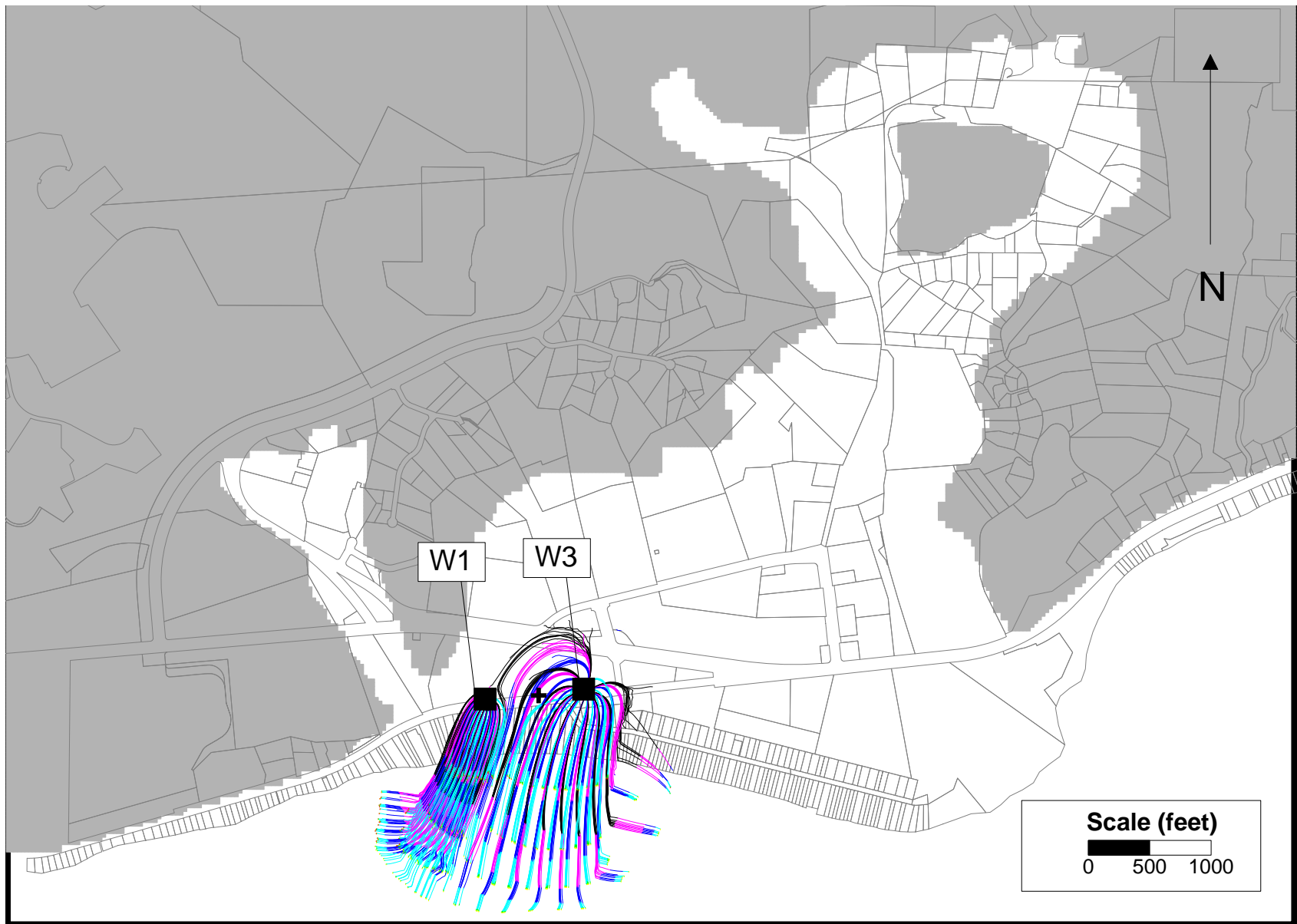


Figure 3.23 - Particle tracking from optimized injection sites representing Phase 2 conditions.

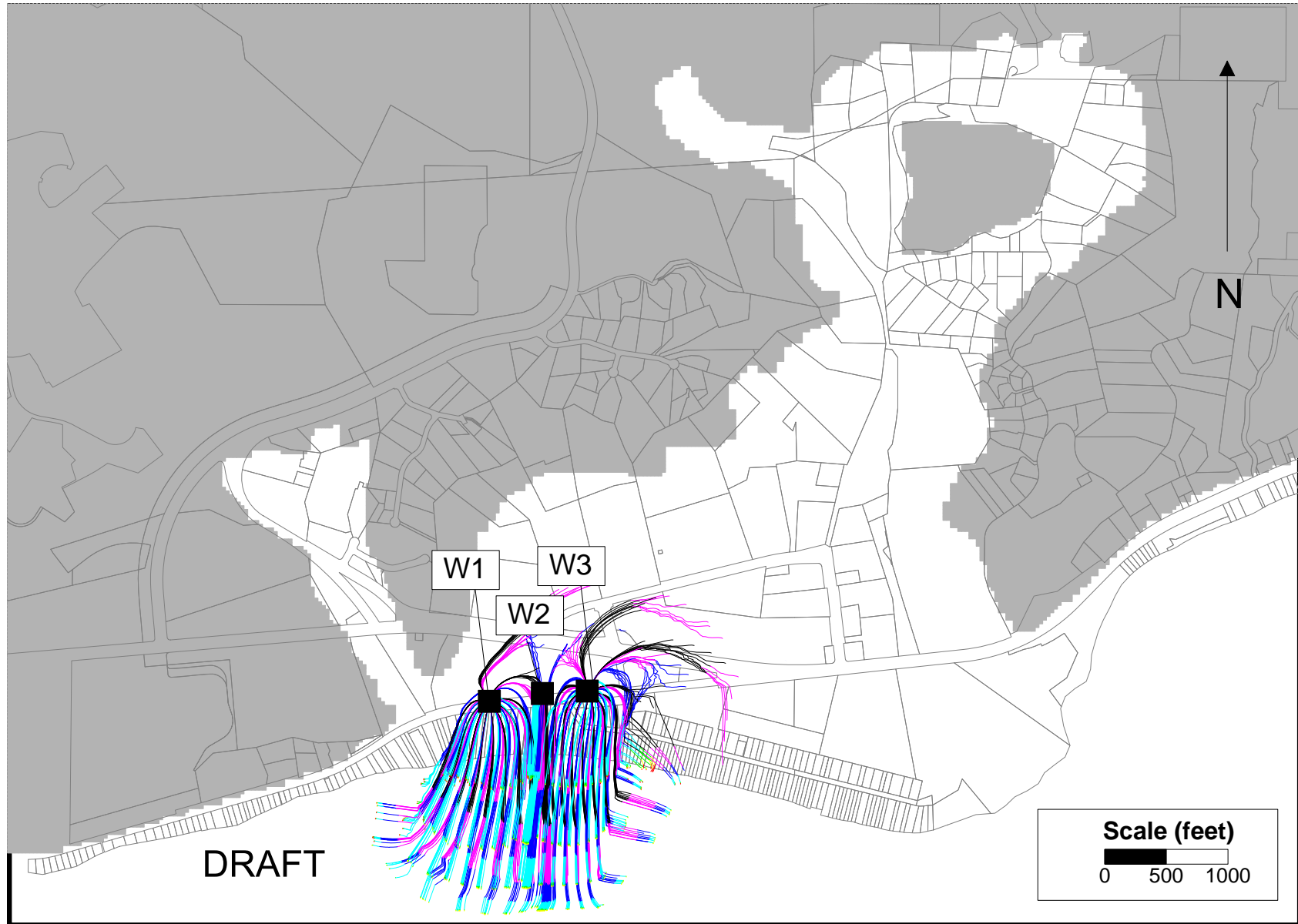


Figure 3.24 - Particle tracking from optimized injection sites representing Phase 3 conditions.

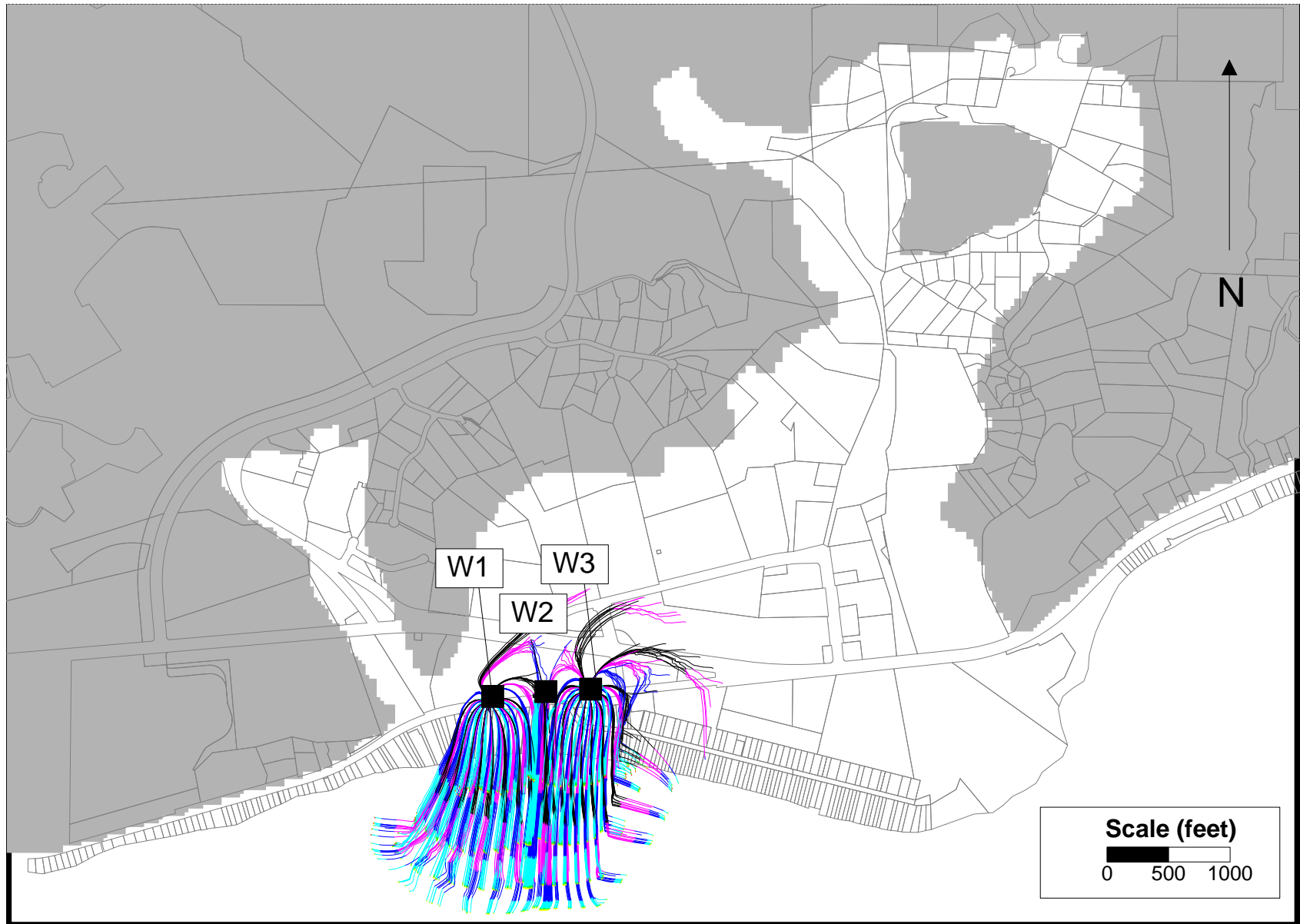


Figure 3.25 - Particle tracking from optimized injection sites representing Phase 3 conditions with a portion, 50,000 gallons per day, being injected into Winter Canyon.



Figure 3.26 - Particle tracking from optimized injection sites representing Phase 3 conditions with a portion, 100,000 gallons per day, being injected into Winter Canyon.

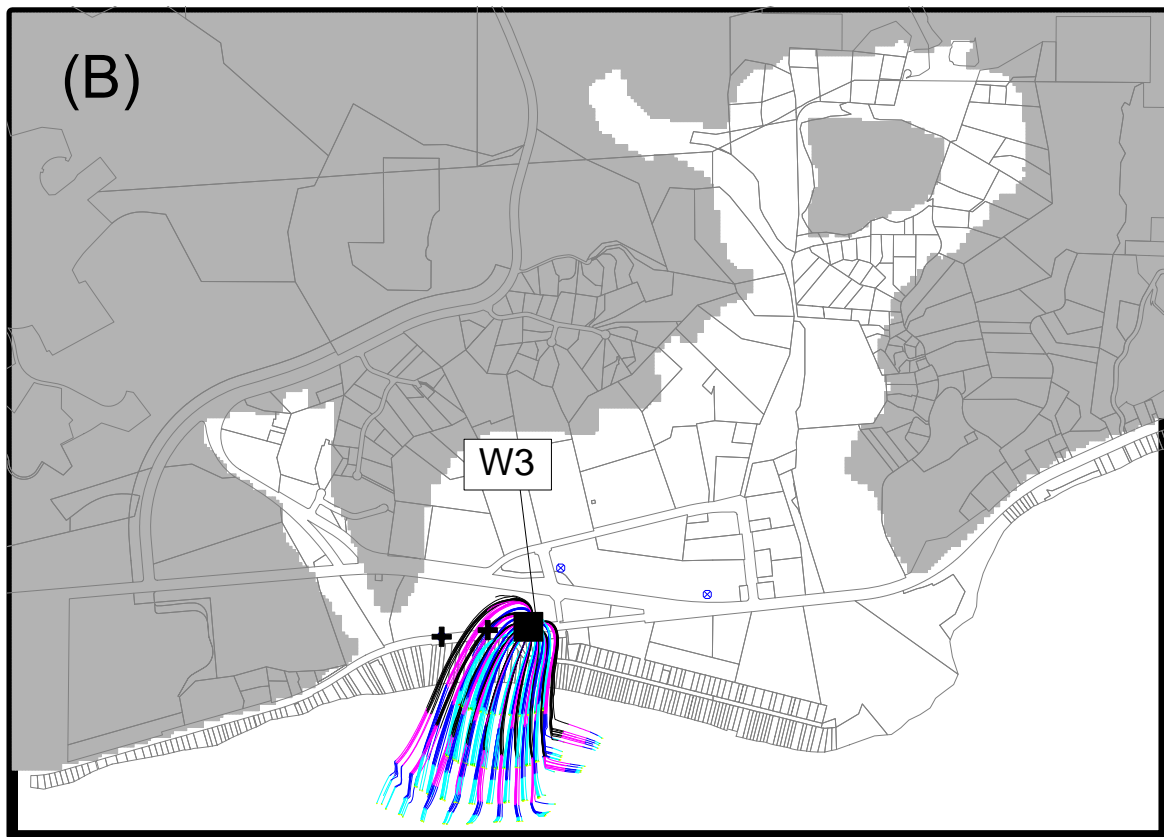
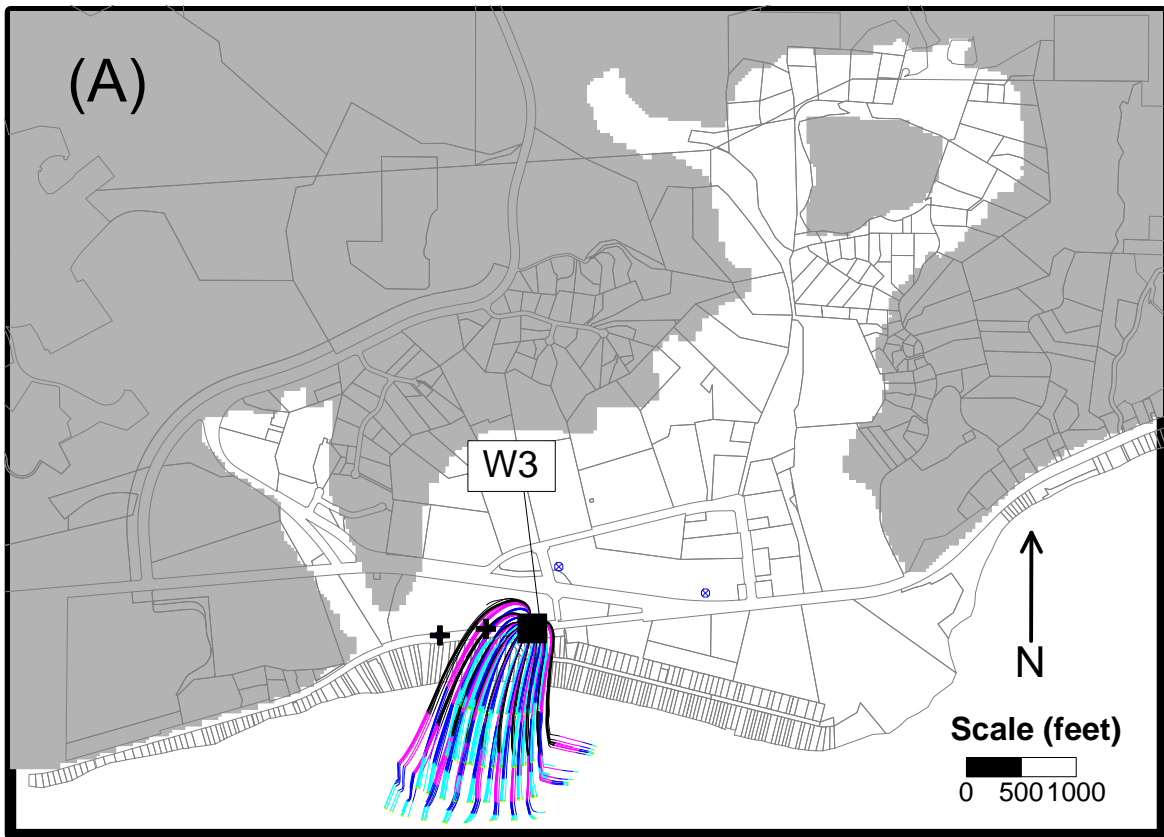


Figure 3.27 - Maps showing comparison between Phase 1 injection (311,135 g/d), for the base run (A) and the deep channel conductivity decreased by 10 percent (B).

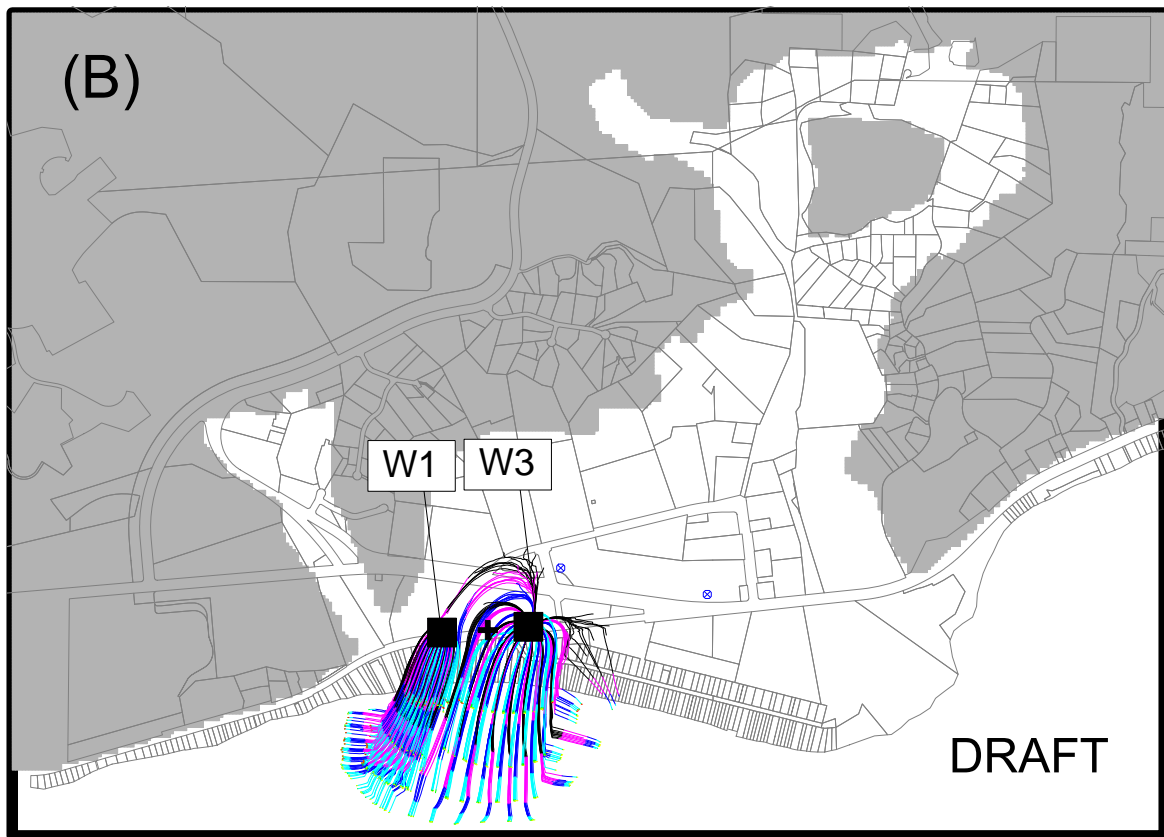
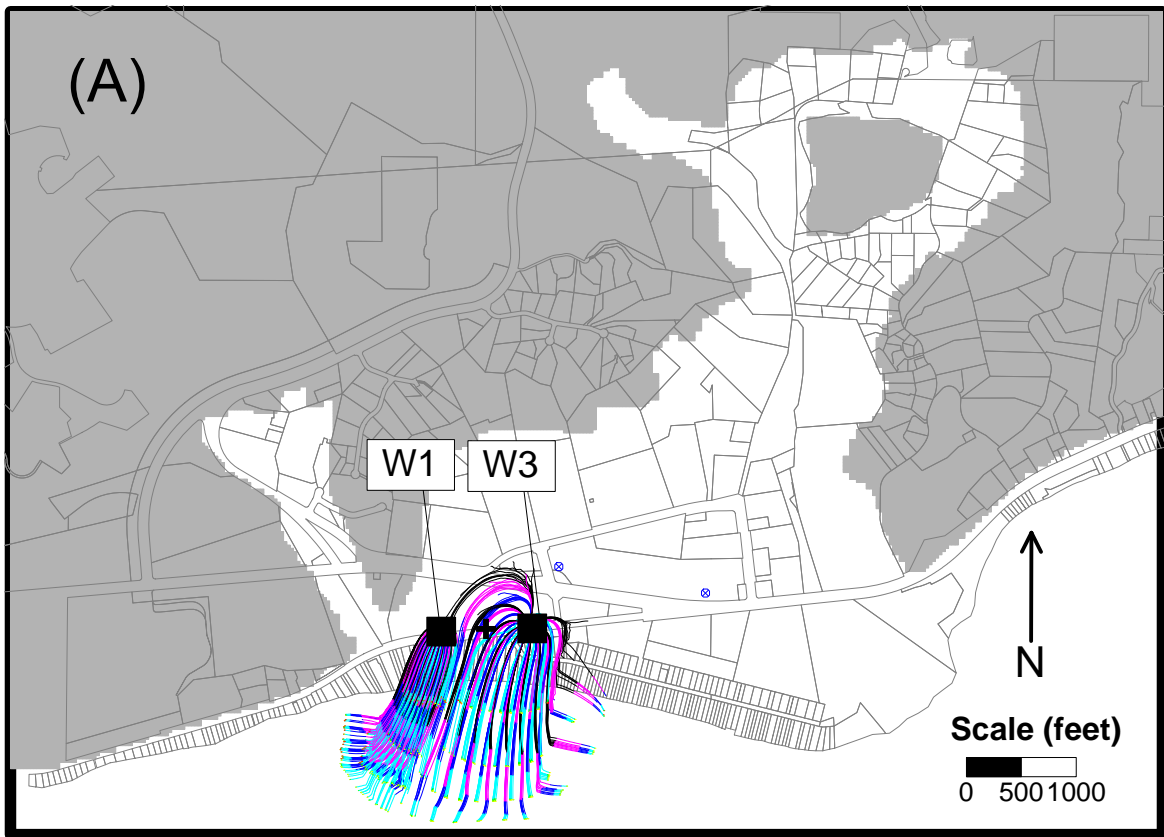


Figure 3.28 - Maps showing comparison between Phase 2 injection (497,642 g/d), for the base run (A) and the deep channel conductivity decreased by 10 percent (B).

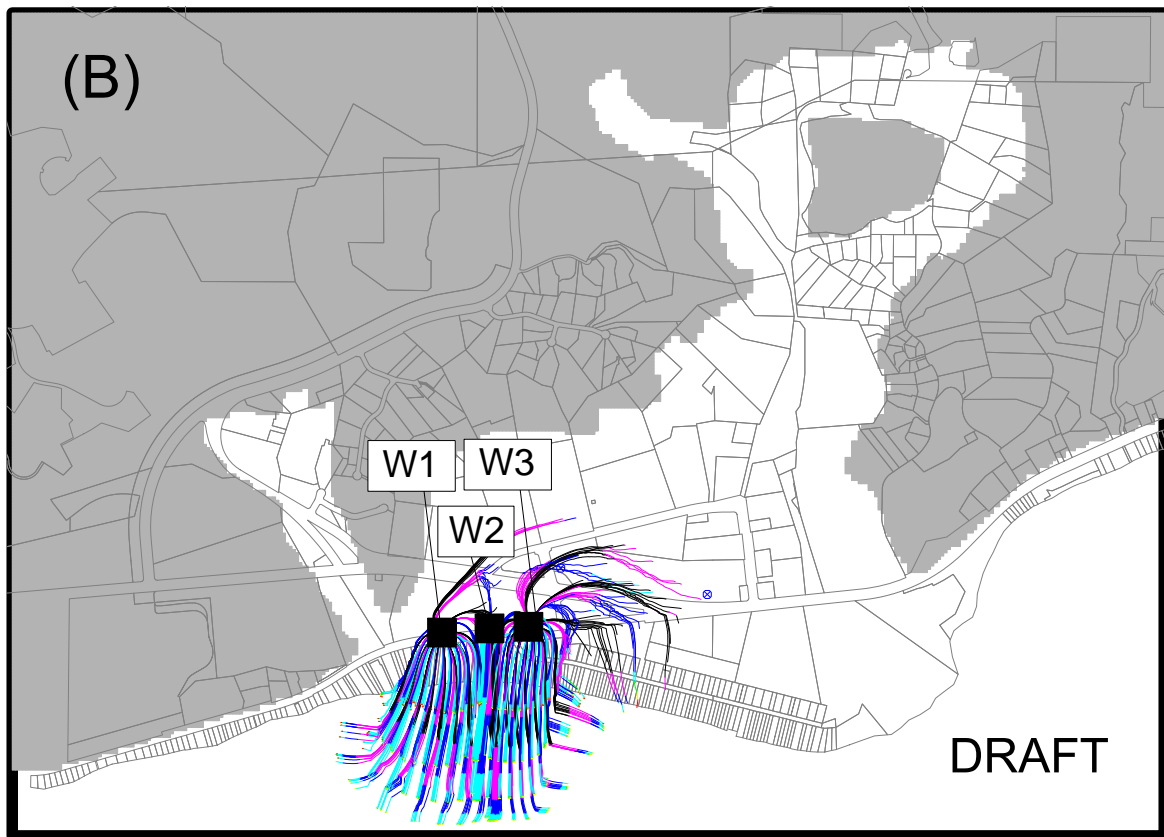
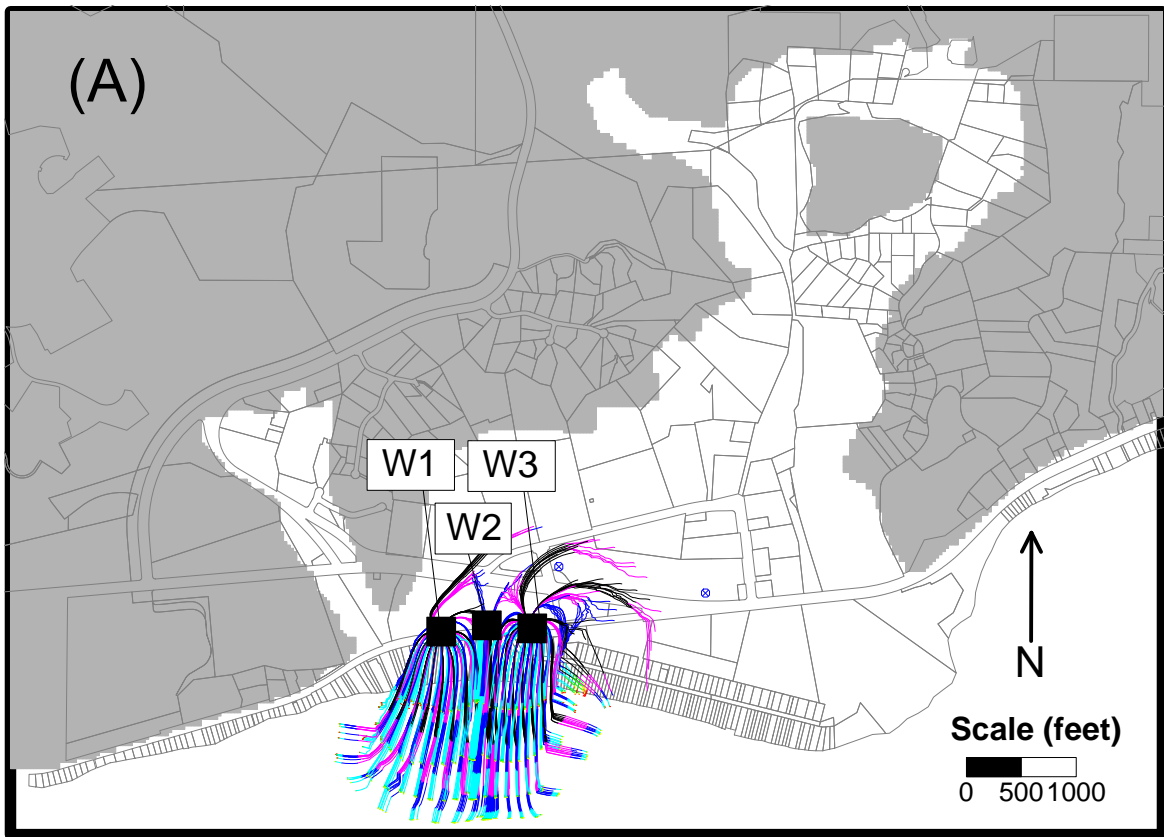


Figure 3.29 - Maps showing comparison between Phase 3 injection (611,655 g/d), for the base run (A) and the deep channel conductivity decreased by 10 percent (B).

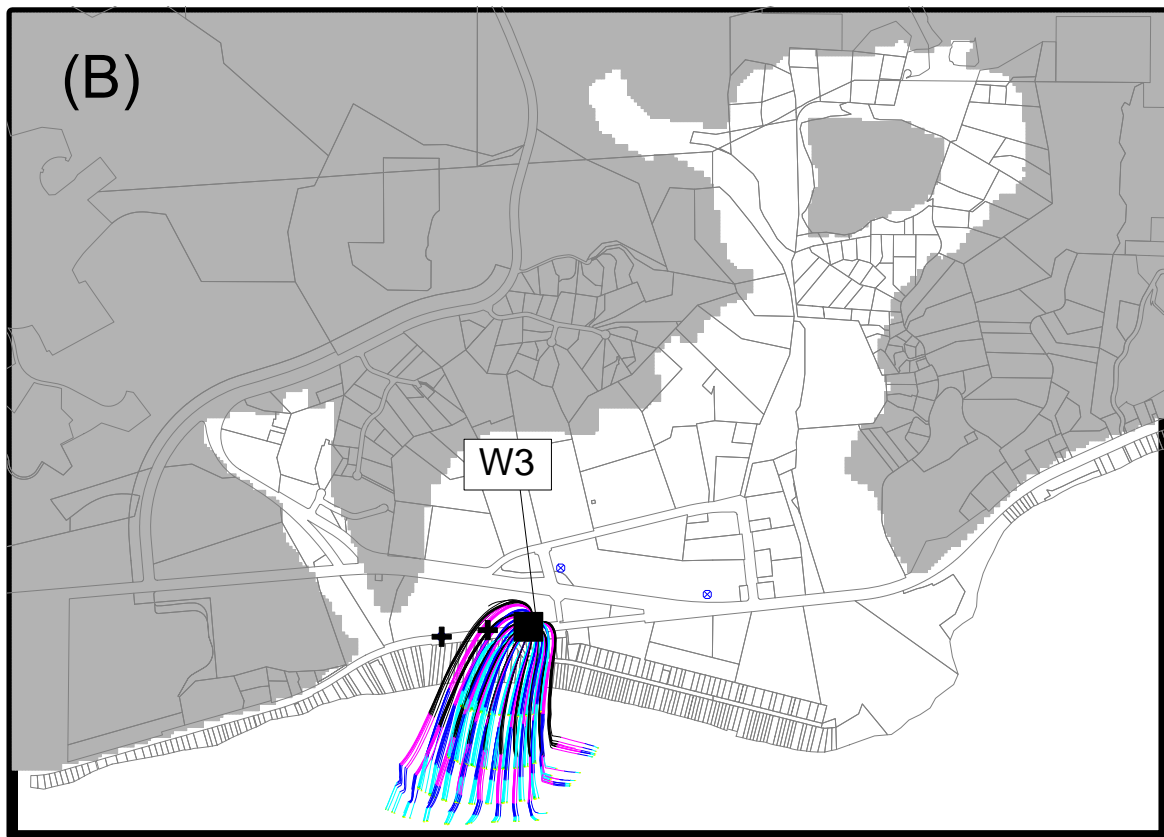
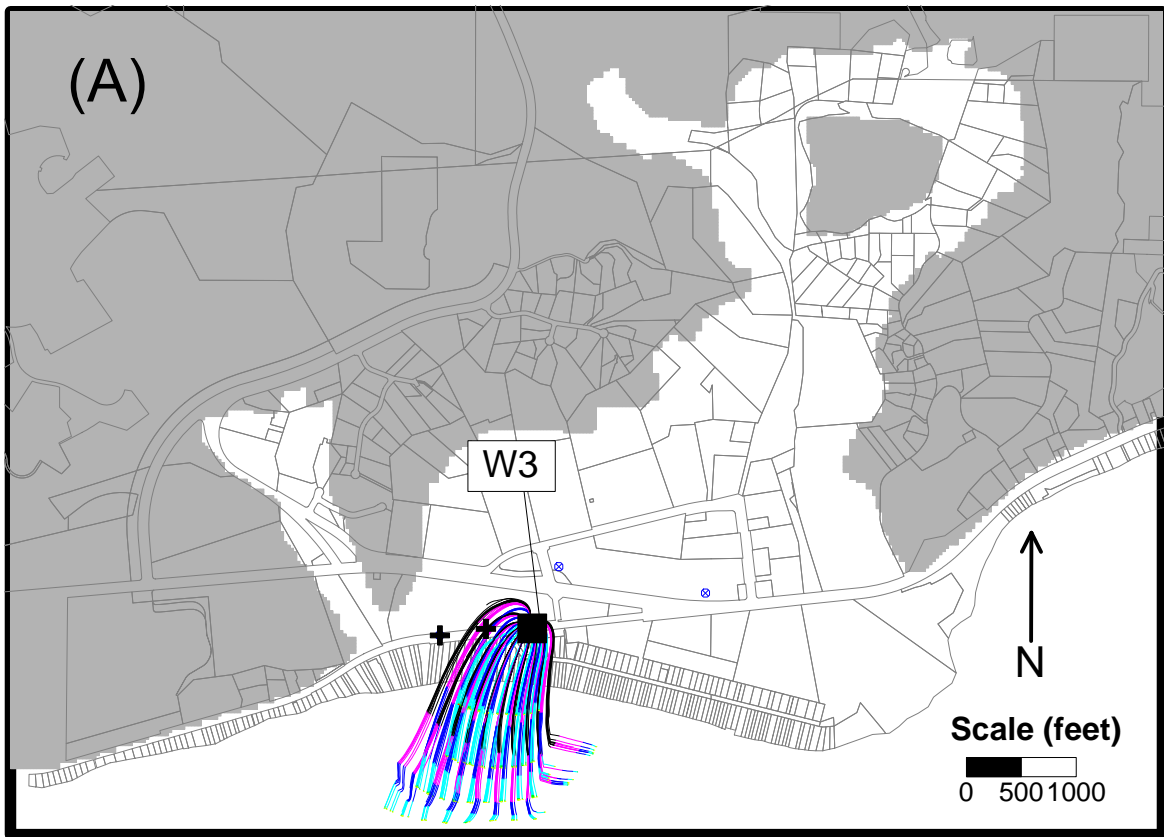


Figure 3.30 - Maps showing comparison between Phase 1 injection (311,135 g/d), for the base run (A) and the low permeability unit vertical conductivity increased by a factor of 2 (B).

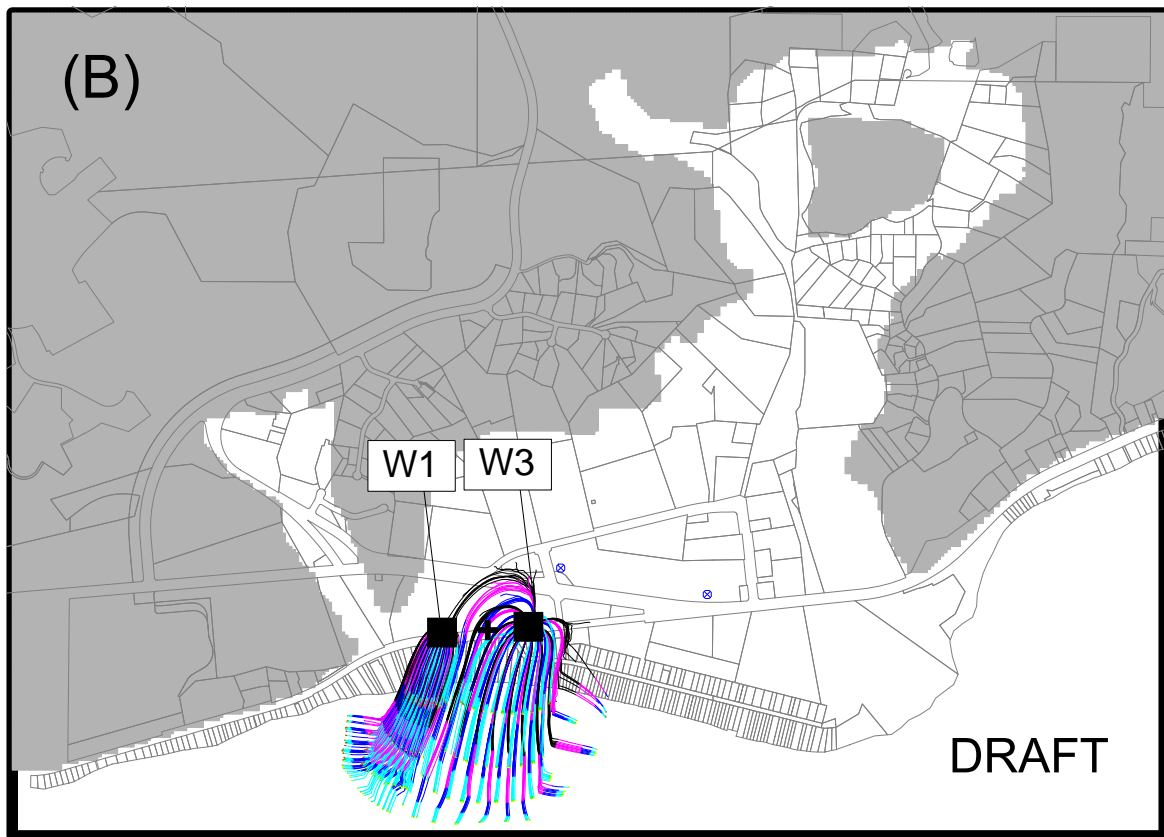
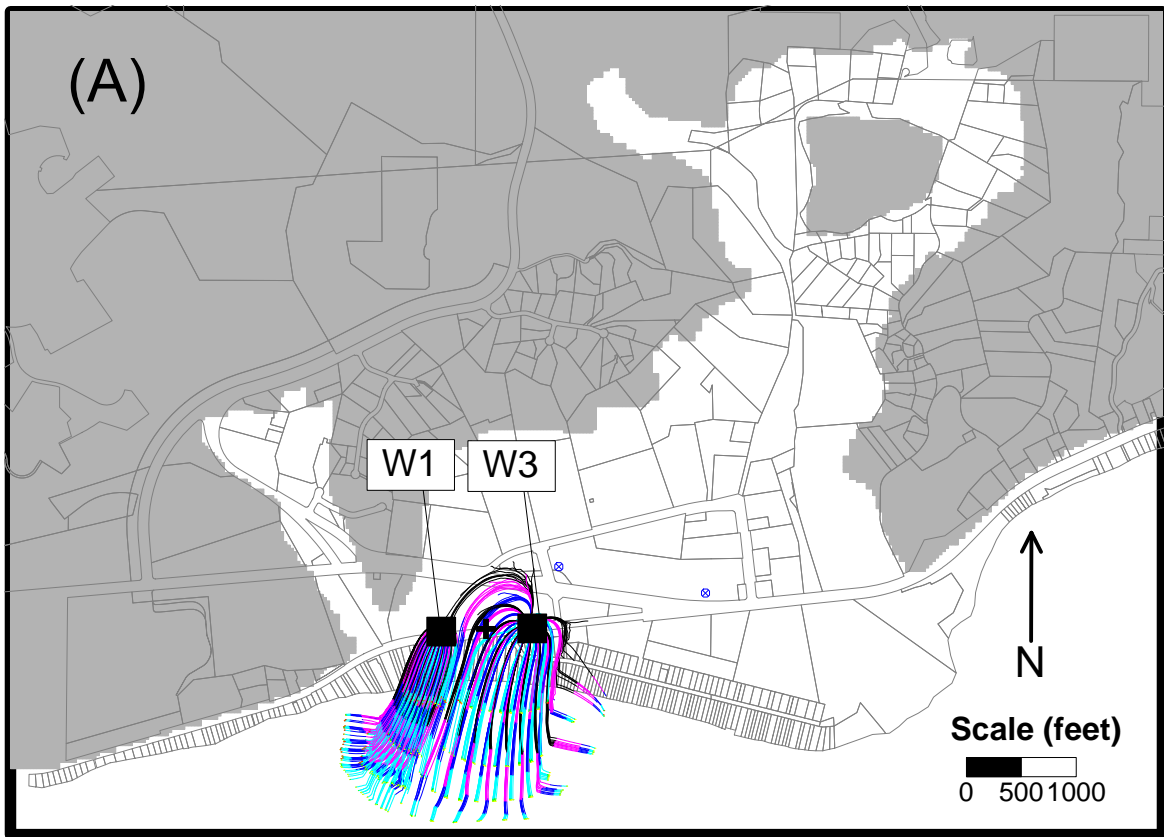


Figure 3.31 - Maps showing comparison between Phase 2 injection (497,642 g/d), for the base run (A) and the low permeability unit vertical conductivity increased by a factor of 2 (B).

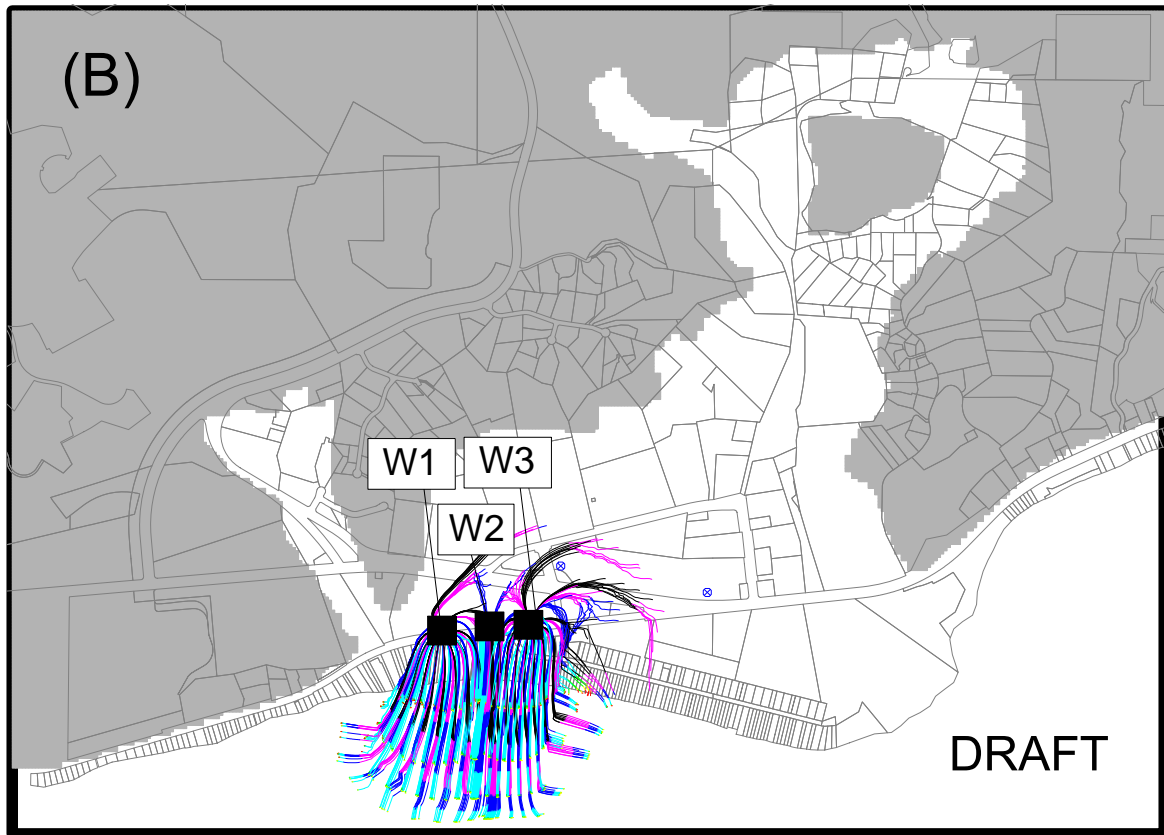
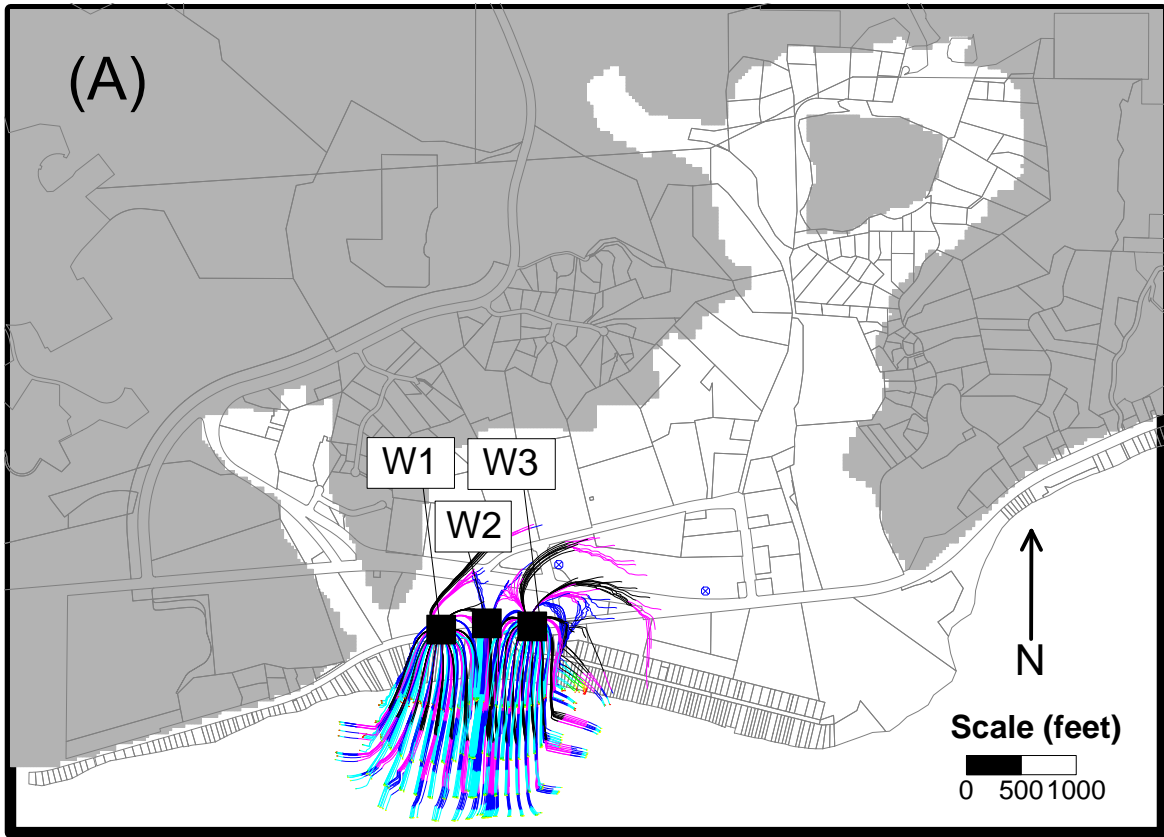


Figure 3.32 - Maps showing comparison between Phase 3 injection (611,655 g/d), for the base run (A) and the low permeability unit vertical conductivity increased by a factor of 2 (B).

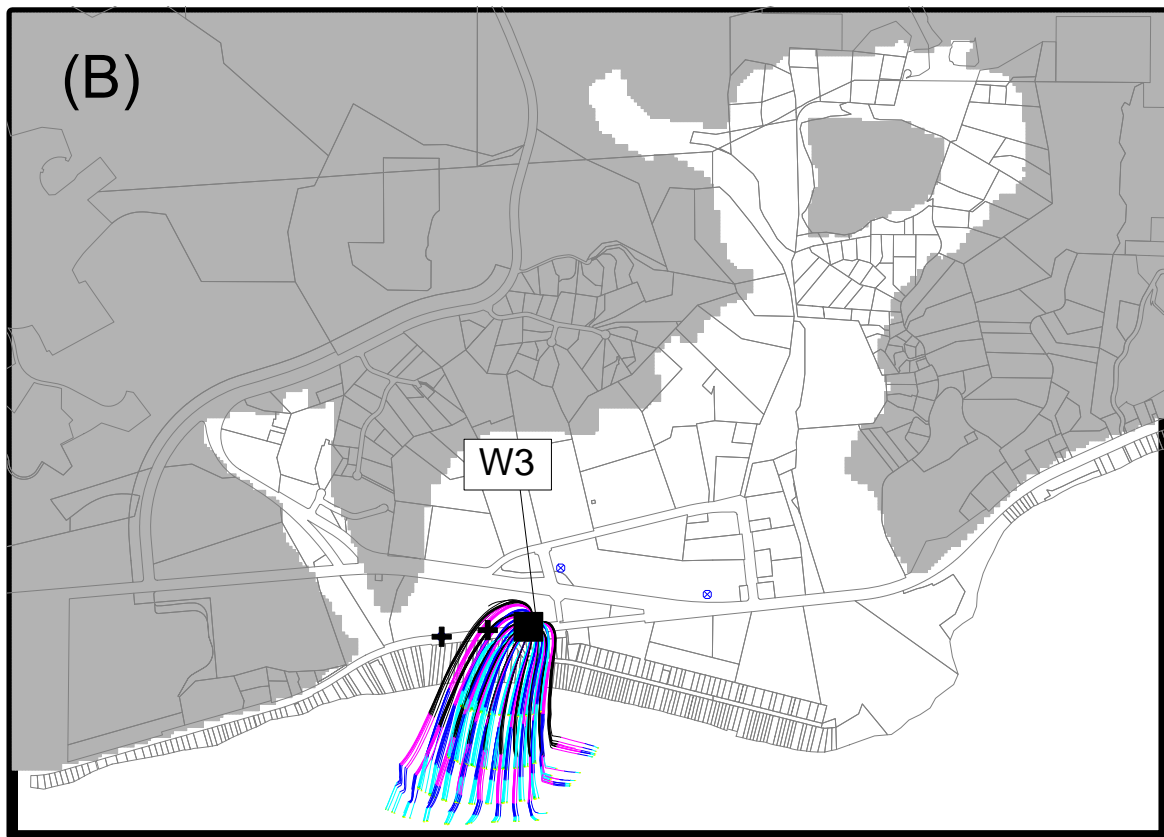
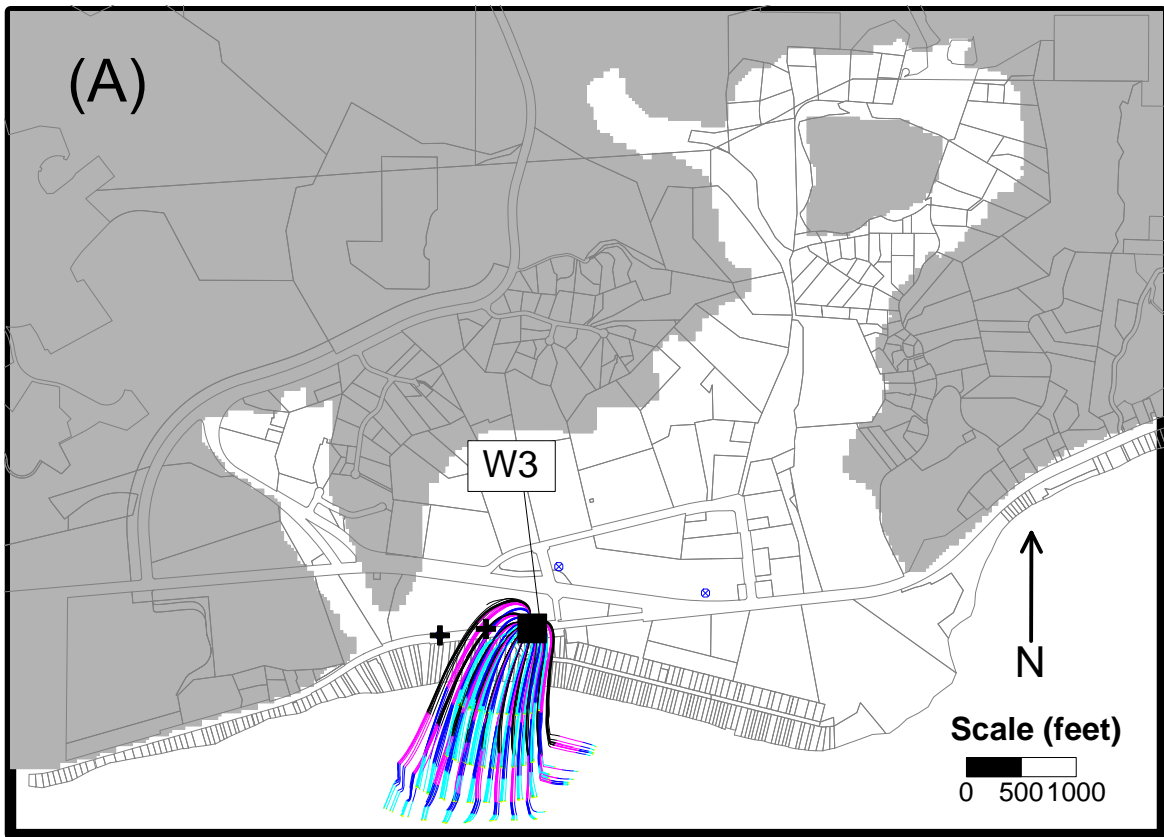


Figure 3.33 - Maps showing comparison between Phase 1 injection (311,135 g/d), for the base run (A) and increasing precipitation recharge by 10 percent (B).

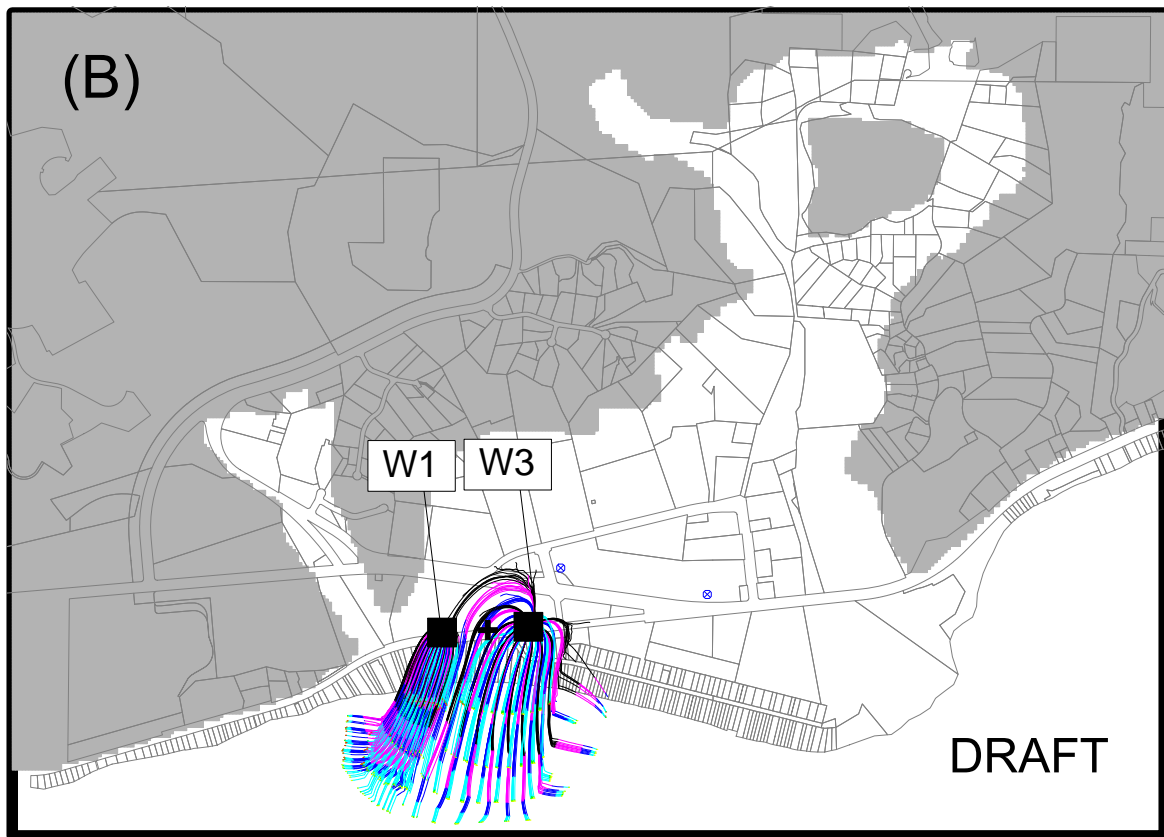
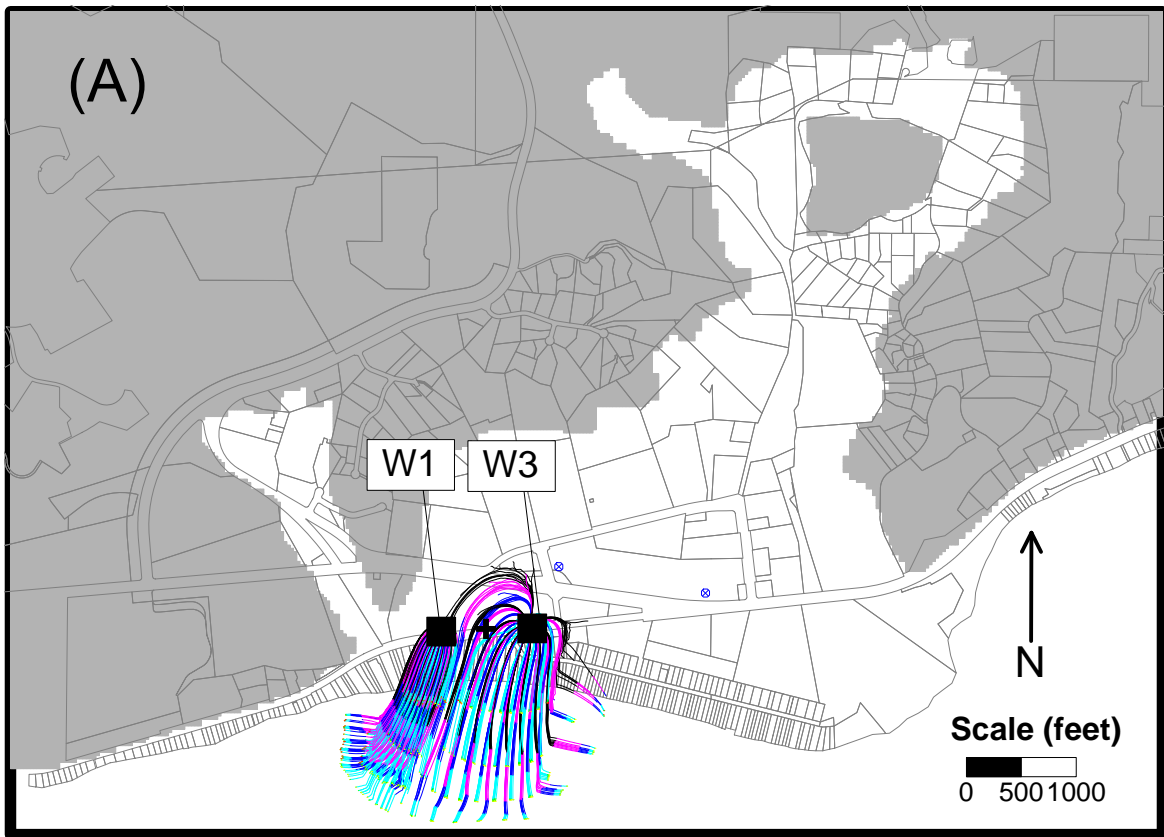


Figure 3.34 - Maps showing comparison between Phase 2 injection (497,642 g/d), for the base run (A) and increasing precipitation recharge by 10 percent (B).

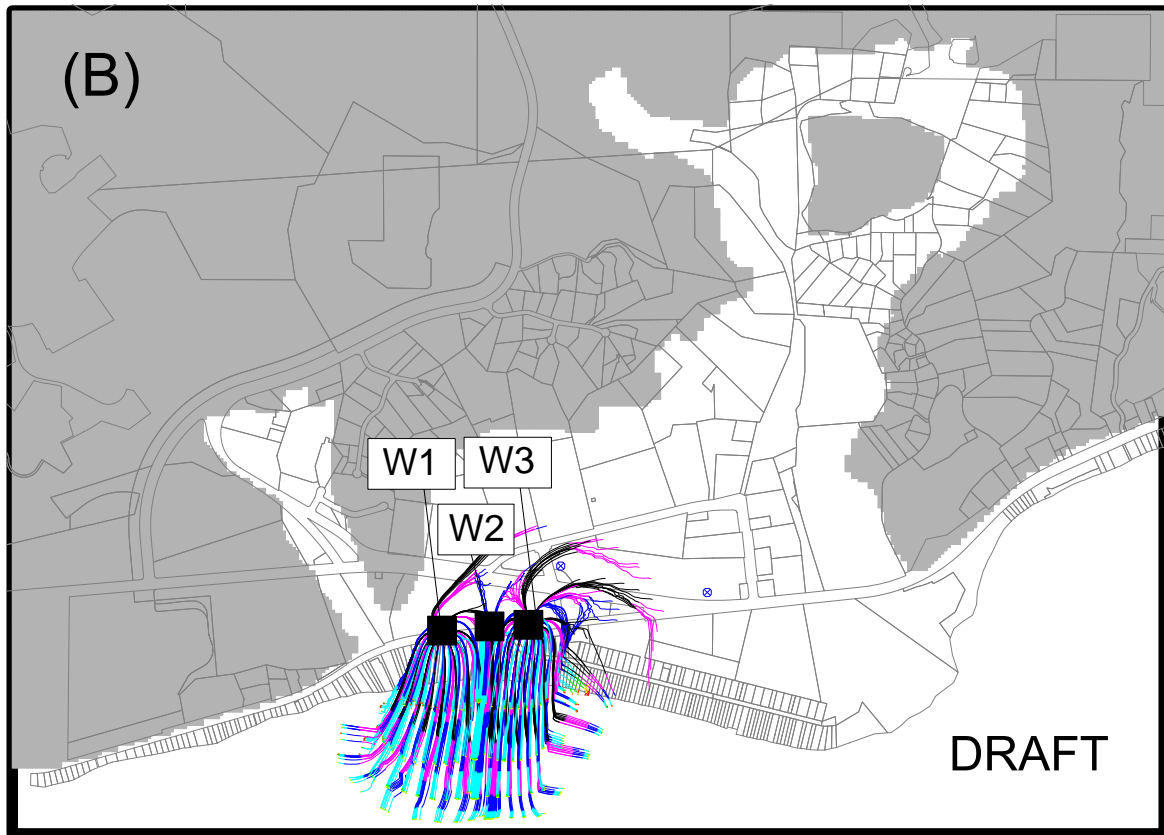
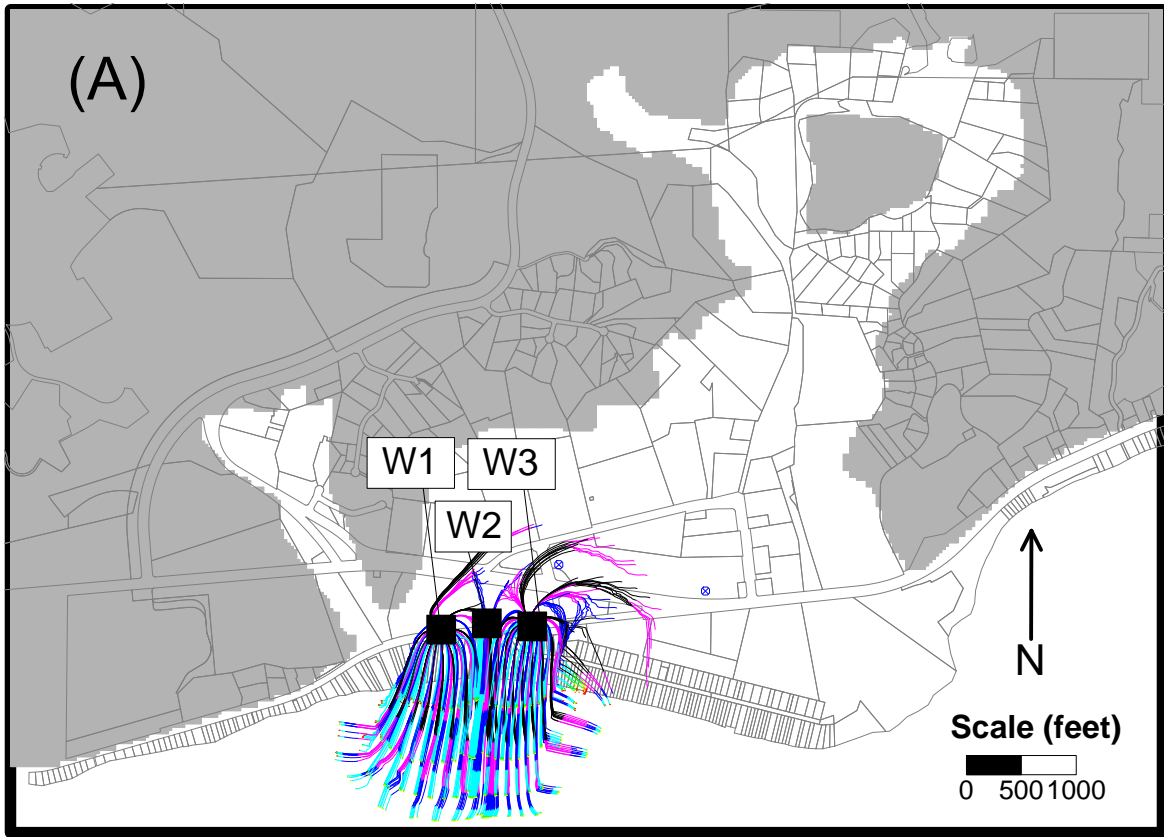


Figure 3.35 - Maps showing comparison between Phase 3 injection (611,655 g/d), for the base run (A) and increasing precipitation recharge by 10 percent (B).